

## REVIEW ARTICLE

[View Article Online](#)  
[View Journal](#) | [View Issue](#)

## Metallic anodes for next generation secondary batteries

Cite this: *Chem. Soc. Rev.*, 2013, **42**, 9011

Hansu Kim,<sup>a</sup> Goojin Jeong,<sup>b</sup> Young-Ukg Kim,<sup>c</sup> Jae-Hun Kim,<sup>d</sup> Cheol-Min Park<sup>e</sup> and Hun-Joon Sohn<sup>\*f</sup>

Received 31st May 2013

DOI: 10.1039/c3cs60177c

[www.rsc.org/csr](http://www.rsc.org/csr)

Li-air(O<sub>2</sub>) and Li–S batteries have gained much attention recently and most relevant research has aimed to improve the electrochemical performance of air(O<sub>2</sub>) or sulfur cathode materials. However, many technical problems associated with the Li metal anode have yet to be overcome. This review mainly focuses on the electrochemical behaviors and technical issues related to metallic Li anode materials as well as other metallic anode materials such as alkali (Na) and alkaline earth (Mg) metals, including Zn and Al when these metal anodes were employed for various types of secondary batteries.

### 1. Introduction

With increasing demands for clean and renewable energy, tremendous efforts have been devoted to developing new materials for solar cells, secondary batteries, fuel cells, and electrical double-layer capacitors. Among these power sources, Li-ion batteries have been successfully implemented in most portable electronic devices, such as cellular phones, computers, and digital cameras. Li-ion battery sales reached more than 11 billion dollars in 2011.<sup>1</sup> Although the usage of Li-ion batteries has been expanded into larger units, including several types of electric vehicles (EVs, hybrid, or plug-in EVs), robots, power tools, and electric power storage units, demand is

<sup>a</sup> Department of Energy Engineering, Hanyang University, Seoul, 133-791, Korea

<sup>b</sup> Advanced Batteries Research Center, Korea Electronics Technology Institute, Seongnam, Gyeonggi, 463-816, Korea

<sup>c</sup> Battery Development Team, Samsung SDI Co., LTD., Cheonan, Chungnam, 330-300, Korea

<sup>d</sup> School of Advanced Materials Engineering, Kookmin University, Seoul 136-702, Republic of Korea

<sup>e</sup> School of Advanced Materials and System Engineering, Kumoh National Institute of Technology, Gumi, Gyeongbuk 730-701, Republic of Korea

<sup>f</sup> Department of Materials Science and Engineering, Seoul National University, Seoul, 151-744, Korea. E-mail: hjsohn@snu.ac.kr; Tel: +82-2-880-7226



Hansu Kim

*Hansu Kim received his PhD in mineral and petroleum engineering from Seoul National University, Korea, in 2000. He joined the Energy Lab. of Samsung Advanced Institute of Technology as a member of research staff in 2001 and moved to Hanyang University in 2011. Currently he is an associate professor in the Department of Energy Engineering at Hanyang University. His research is mainly focused on nanostructured alloy-type anode materials for next generation lithium secondary batteries and alkali metal(Li/Na) based rechargeable batteries.*



Goojin Jeong

*Goojin Jeong is a research professional at Advanced Batteries Research Centre, Korea Electronics Technology Institute (KETI). Previously, he was a research professor at the Kumho National Institute of Technology (2010–2011) and a senior researcher at Samsung SDI (2003–2010) for developing advanced Li secondary batteries. He received his PhD from Seoul National University in 2001, and did his postdoctoral work at the Arizona State University (2002–2003). His research interests involve electrochemical behaviour of materials related to energy conversion and storage systems. Recently he is focusing on alternative anode materials for LiB and post-LiB systems for next generation.*

continuously increasing for storage devices with higher gravimetric and volumetric energy density for EVs with long ranges (of approximately 500 km) and large energy storage systems for load-leveling applications. Current Li-ion batteries cannot meet the requirements for these applications. Detailed material and technical issues of the Li-ion batteries related to these applications have been discussed in other works.<sup>2–4</sup>

Recently, much effort has been devoted to the development of Li-air(O<sub>2</sub>) or Li-S batteries for EVs and large electricity storage systems, since these batteries have much higher gravimetric and volumetric energy densities than conventional Li-ion batteries. Fig. 1 illustrates the basic principles of metal-air(O<sub>2</sub>) or metal-S battery systems. Anode materials include Li, Na, Mg, Al, or Zn metals. The cathodes consist of catalysts for O<sub>2</sub> reduction or sulfur, both of which include porous networks of conducting/supporting agents. Electrolytes can mainly be divided into two groups: non-aqueous organic or aqueous

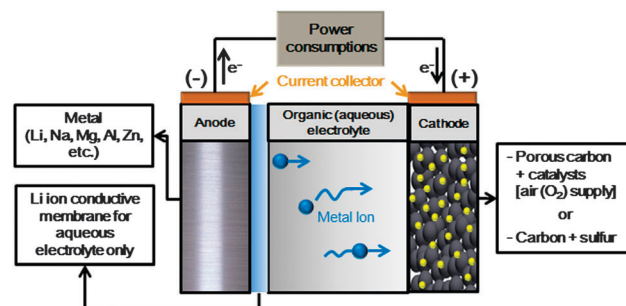


**Fig. 1** Schematic principle of operation for metal–air(O<sub>2</sub>) or metal–sulfur batteries.

electrolytes for metal–air(O<sub>2</sub>) batteries. However, Na–S batteries employ beta alumina solid electrolytes, while liquid Mg–Sb batteries use molten salt electrolytes (MgCl<sub>2</sub>–KCl–NaCl).



**Young-Ugk Kim**

Young-Ugk Kim received his PhD degree from the School of Materials Science and Engineering of Seoul National University in 2005 under the supervision of Professor Hun-Joon Sohn. He worked as a Postdoctoral Research Associate at the University of Utah studying nanoparticle synthesis using high temperature processes. His research interests are in the secondary battery electrode material development

and, since 2006, he has been working as a Senior Researcher of Samsung SDI, the world's leading lithium secondary battery company.



**Jae-Hun Kim**

Jae-Hun Kim is currently an Assistant Professor at Kookmin University. He received his BS, MS, and PhD degrees from the Department of Materials Science and Engineering from Seoul National University (Korea). He did his postdoctoral work at the University of Idaho (2007–2008) and the National Renewable Energy Laboratory of the United States (2008–2010). He also worked as a senior researcher at Korea Electronics Technology Institute (2010–2013). His current research interests are focused on synthesis and electrochemical analysis of key materials for electrochemical energy storage devices such as lithium batteries, flow batteries, and supercapacitors.



**Cheol-Min Park**

Cheol-Min Park is an assistant professor at the School of Advanced Materials and System Engineering, Kumoh National Institute of Technology (KIT). He received his MS (2005) and PhD (2009) from the Department of Materials Science & Engineering of Seoul National University. He also worked as a researcher at LG Chem. Ltd. Battery Research Institute (2005–2006) and Environmental Energy Technologies Division of Lawrence Berkeley

National Laboratory (2009–2010). His research interests are focused on synthesis and investigation of new alternative electrode materials for rechargeable Li-, Na-, and Mg-based battery systems.



**Hun-Joon Sohn**

Hun-Joon Sohn received his BS and MS degrees in metallurgical engineering from Seoul National University. He also earned PhD from the University of Utah in Salt Lake City, USA, in 1980. He did his postdoctoral work at the same university and joined Seoul National University in 1982. Currently he is a Professor in the Department of Materials Science and Engineering at SNU. His research interests involve electrochemical behavior of materials under various conditions and recently he has mainly focused on the development and characterization of anode materials for Li secondary batteries.

Fig. 1 shows the Li-ion conducting membrane normally required for aqueous electrolytes to prevent direct contact between the Li metal anode and water in Li-air(O<sub>2</sub>) batteries. The reaction chemistries involved for O<sub>2</sub> and sulfur electrodes vary depending on the electrolytes, and have been discussed in detail in recent reviews.<sup>5,6</sup> In principle, Li metal dissolves to form Li ions on the anodic side, which move to the cathodic electrode to react with oxygen to form Li<sub>2</sub>O<sub>2</sub> (Li<sub>2</sub>O) in organic electrolytes (or LiOH in aqueous electrolytes) for Li–O<sub>2</sub> batteries. In Li–S batteries, Li reacts with sulfur to form Li<sub>2</sub>S as the final product during discharge. A reverse reaction should occur during the charging step. In metal–air(O<sub>2</sub>) batteries, metal dissolves in the alkaline aqueous electrolyte at the anode, and OH<sup>−</sup> ions are generated in the cathode due to the reduction of O<sub>2</sub>. In this case, OH<sup>−</sup> ions shuttle between the cathode and the anode to form a solid oxide or hydroxide product at the anode as the final phase during discharge.

Table 1 provides the theoretical cell voltage with the specific energy (energy per unit weight) and energy density (energy per unit volume) for various metal–air(O<sub>2</sub>) or metal–S batteries. At 3582 W h kg<sup>−1</sup>, the Li–air(O<sub>2</sub>) battery supplies the highest theoretical specific energy, which is 10 times that of current Li-ion batteries. Zn–air(O<sub>2</sub>) batteries (which form ZnO as the final product) deliver the largest theoretical energy density of 6091 W h l<sup>−1</sup>, due to the relatively high density of Zn metal.

In this review, the material problems associated with metallic anodes in metal–air(O<sub>2</sub>) or metal–S batteries are discussed, since the aforementioned reviews were mainly focused on air(O<sub>2</sub>) or S electrodes. Perspectives on the next generation of high-energy-density secondary batteries are provided.

**Table 1** Theoretical cell voltage with specific energy and energy density for various metal–O<sub>2</sub> or metal–sulfur batteries

Battery system	Voltage (V)	Specific energy (W h kg <sup>−1</sup> )	Energy density (W h l <sup>−1</sup> )
Li-ion <sup>5</sup>	3.8	387	1015
Zn–air <sup>5</sup>	1.65	1086	6091 <sup>a</sup>
Li–O <sub>2</sub> (organic electrolyte) <sup>5</sup>	3.0	3505	3436 <sup>b</sup>
Li–O <sub>2</sub> (aqueous electrolyte) <sup>5</sup>	3.2	3582	2234 <sup>c</sup>
Li–S <sup>5</sup>	2.2	2567	2199 <sup>d</sup>
Mg–air	3.09	2840	3859 <sup>h</sup>
Al–air	2.71	2793	3679
Na–air	2.33	1605 <sup>e</sup>	1661
Na–S	2.1	790	972 <sup>f</sup>
Na–NiCl <sub>2</sub>	2.57	785	2639 <sup>g</sup>
Mg–Sb(liqu.)	0.51 <sup>i</sup>	683 <sup>i</sup>	1006 <sup>i</sup>

<sup>a</sup> Based on the volume of ZnO at the end of discharge. <sup>b</sup> Based on the sum of the volume of Li at the beginning and Li<sub>2</sub>O<sub>2</sub> at the end of discharge. <sup>c</sup> Based on the sum of the volume of Li + H<sub>2</sub>O consumed and LiOH at the end of discharge. <sup>d</sup> Based on the sum of the volume of Li at the beginning and Li<sub>2</sub>S at the end of discharge. <sup>e</sup> Based on (Na + Na<sub>2</sub>O<sub>2</sub>). <sup>f</sup> Based on the sum of the volume of Na at the beginning and Na<sub>2</sub>S<sub>3</sub> at the end of discharge. <sup>g</sup> Based on the sum of the volume of 2 moles of Na and NiCl<sub>2</sub> at the beginning. <sup>h</sup> Based on the sum of the volume of Mg at the beginning and Mg(OH)<sub>2</sub> at the end of discharge.

<sup>i</sup> Based on the result reported in the literature and the sum of the weight/volume of the final composition (Mg<sub>0.12</sub>Sb<sub>0.88</sub>) at the end of discharge.

## 2. Metallic lithium (Li) electrode

### 2.1 Technical issues of Li anode

**2.1.1 Problems of Li anode.** Although metallic Li has the largest theoretical capacity (3860 mA h g<sup>−1</sup>), Li electrodes suffer some drawbacks as an anode material for Li secondary batteries. It is generally known that electrodeposited Li shows a dendritic/granular morphology when the metallic Li electrode is charged.<sup>8,9</sup> Fig. 2 shows typical dendritic Li morphology taken from an Li/gel polymer electrolyte/LiMn<sub>2</sub>O<sub>4</sub> cell after one cycle.<sup>10</sup> The dendritic Li formed may come into direct contact with the positive electrode, which causes an internal short circuit and spontaneous high-rate discharge of the battery, resulting in rapid heating and explosion of the cell.<sup>11–13</sup> Granular forms or aggregates of metallic Li particles can also lead to internal short-circuits of the cell, because some of the aggregates may detach from the Li electrode, and the isolated Li particles in the electrolyte move to the positive electrode. The repeated charge and discharge (Li plating/stripping) of an Li electrode degrades the thermal stability of the battery.<sup>8,13</sup>

Sacken *et al.* employed accelerated rate calorimetry (ARC) to a metallic Li electrode battery,<sup>12</sup> and Fig. 3 shows the ARC exotherms of a cycled Li–MnO<sub>2</sub> AA-size cell. The ARC exotherms indicated that the self-heating rate significantly increased with the cycle number, probably due to the increase in the surface area of the Li electrode. Although the pristine cell has good thermal stability, repeated plating and dissolution of Li metal can make the cell more sensitive to thermal abuse, thus degrading the thermal stability of the cell. Moli Energy, a Canadian company, commercialized rechargeable Li batteries composed of metallic Li as an anode and MoS<sub>2</sub> as a cathode in the late 1980s.<sup>14,15</sup> Although Li–MoS<sub>2</sub> rechargeable battery systems showed high energy density and relatively good cycle performance, safety incidents occurred in the field, eventually resulting in a recall of all cellular phone battery packs.<sup>15,16</sup>

Poor cycling efficiency is another technical issue with metallic Li anodes. Li is a highly active metal that is prone to reacting with non-aqueous solvents and water.<sup>17,18</sup> However, electrochemical deposition and dissolution of metallic Li is possible in some

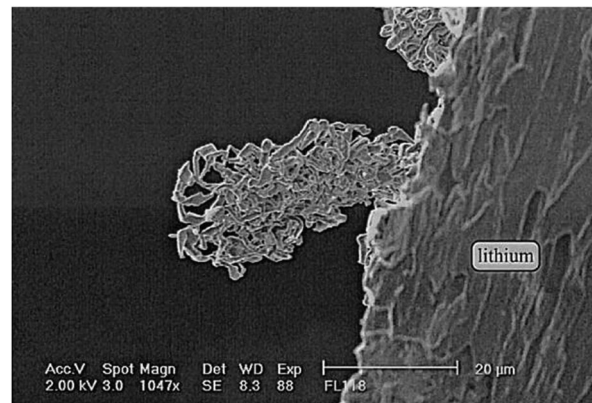


**Fig. 2** Dendritic Li formed in a Li battery after charge at 2.2 mA cm<sup>−2</sup> (Science Direct, reprinted with permission)<sup>10</sup>

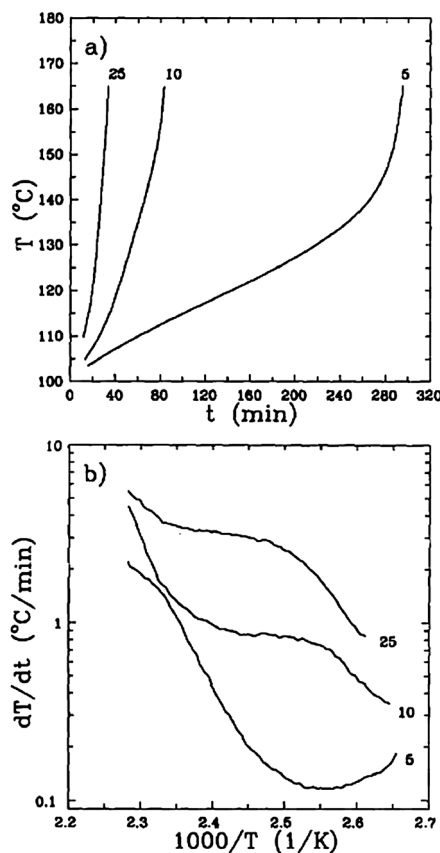


**Fig. 3** ARC exotherms of cycled Li–MnO<sub>2</sub> cells starting from 100 °C: (a) temperature vs. time and (b) the corresponding Arrhenius plot ( $dT/dt$  vs.  $1000/T$ ) (Science Direct, reprinted with permission).<sup>12</sup>

non-aqueous electrolytes.<sup>19,20</sup> Peled suggested that Li reacts with the electrolyte to form a protective film called the solid electrolyte interphase (SEI), which prevents further reaction of Li metal with the organic electrolyte.<sup>21</sup> In general, the SEI thin film formed on the Li surface conducts Li<sup>+</sup>, but acts as an electronic insulator. Much attention has been devoted to identifying the composition and microstructure of SEIs using various analytical techniques, such as X-ray photoelectron spectroscopy (XPS),<sup>22–24</sup> Fourier transform infrared spectroscopy,<sup>25</sup> Raman spectroscopy,<sup>26,27</sup> and atomic force microscopy (AFM).<sup>28,29</sup> The chemical composition and microstructure of the SEI on an Li electrode are strongly correlated with the composition of the non-aqueous electrolyte, which is made with an organic solvent and Li salt.<sup>8,13,30,31</sup> It is generally accepted that the SEI on an Li electrode consists of ROLi (R: alkyl group), ROCOOLi, Li<sub>2</sub>CO<sub>3</sub>, and LiX (X: halogen). Aurbach's group extensively studied the SEI formed on the Li surface, and reported that the SEI was composed of multiple layers with various components that depend on the electrolytes, as shown in Fig. 4.<sup>30</sup> Reversible Li deposition and dissolution respectively occur during the charge and discharge processes through these multilayered surface films composed of inorganic and organic Li species. However, the SEI cannot endure the shape and volume changes of the Li electrode, which leads to non-uniform Li deposition and dissolution during cycling. This has been

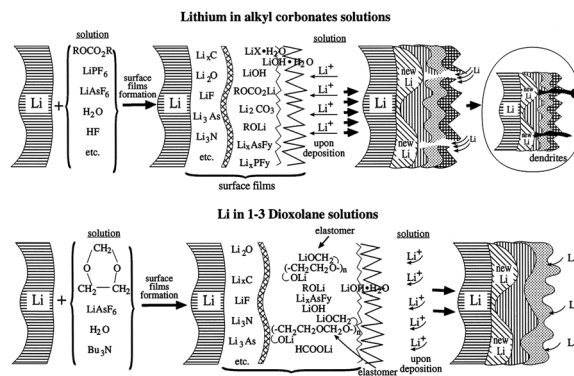


**Fig. 4** Schematic illustration of surface film formation on the Li electrode in alkyl carbonates and the 1,3-dioxolane electrolyte (Science Direct, reprinted with permission)<sup>30</sup>

considered as one of the main reasons for the dendritic growth of Li. Breakdown of the SEI on the Li electrode during cycling leads to the exposure of fresh Li to the electrolyte, and the formation of a new SEI film. This causes further consumption of the bare Li, which decreases the cycling efficiency of the Li electrode. The cycling efficiencies of an Li electrode in commonly used non-aqueous electrolytes, such as alkyl carbonates and ethers with inorganic Li salts, are too low for use in practical rechargeable batteries.<sup>30</sup> Continuous Li consumption during cycling also requires an excess of Li in the battery. For example, the Li–MoS<sub>2</sub> cell by Moli Energy was designed to have a 3-fold excess of Li in the battery, which decreases the energy density.<sup>15</sup> Therefore, in addition to the safety issues of Li metal electrodes, the poor cycle performance should be solved for the commercialization of Li-metal-based rechargeable batteries.

**2.1.2 Key factors for Li electrode.** In order to use metallic Li electrodes for Li secondary batteries, many have focused on the morphological control of electrodeposited Li to suppress dendritic growth, which is affected by the composition of the electrolyte (salt and solvent) and the magnitude of the current density.<sup>32–35</sup>

Most metals are electrodeposited in the dendritic form as the current density reaches the limiting current density ( $i_L$ ),<sup>36,37</sup> indicating that the roughness development in the electrodeposition of metal is governed by the current distribution on the electrode. Arakawa *et al.* reported that the amount of needle-like Li increased when the charge current density of Li/amorphous V<sub>2</sub>O<sub>5</sub> cells increased, suggesting that the applied overpotential during the plating of Li was correlated with the morphology of Li.<sup>32</sup> Recently, Mayers *et al.* studied the reductive deposition of Li cations using a coarse-grained simulation model.<sup>38</sup> They found that the propensity for dendrite formation increased with the applied electrode overpotential, which confirmed the observations by Arakawa *et al.* As mentioned previously, the dendritic morphology of Li unfavorably influences both the safety of Li secondary batteries and the cycle performance. These results suggest that the morphology control of the Li electrode is one of the most important factors for determining the cycle life and reliability of Li secondary batteries. However, the

roughness control of Li during electrodeposition has not been successful to date. Brissot *et al.* reported that Li eventually forms dendrites and spreads out on the electrode at any current density after a certain time.<sup>39</sup> Therefore, complete control of the roughness of Li during cycling is required for the commercialization of Li-metal-based secondary batteries.

Stability of the interphase between Li metal and the electrolyte is also an essential prerequisite for long-term cycle life and safety of the Li electrode, since the breakdown of the SEI during cycling is one of the major reasons for the dendritic formation of Li and successive electrolyte decomposition in the cell. Considering the severe volume changes of Li during cycling, the surface film of the Li electrode should have mechanically robust properties to accommodate the interfacial volume changes during plating and dissolution of Li. In this regard, a variety of strategies to improve the interfacial stability of Li electrodes were investigated, some of which have demonstrated improvements in the cycling efficiency and capacity retention. 1,3-Dioxolane with an LiAsF<sub>6</sub> electrolyte system is one potential approach to significantly improving the interfacial stability of Li electrodes.<sup>40</sup> Aurbach *et al.* reported that the composition of the SEI in this electrolyte consisted of the reduction products of dioxolane, such as HCOOLi and CH<sub>3</sub>CH<sub>2</sub>OCH<sub>2</sub>Li, as well as salt reduction products such as LiF and Li<sub>x</sub>AsF<sub>y</sub>, and oligomers of polydioxolane, which have been known to form by the partial polymerization of 1,3-dioxolane (Fig. 4).<sup>13,30</sup> Since the SEI of a Li electrode contains these elastomers, it can reasonably be expected that the elastomer component renders the interfacial layer more flexible than an SEI composed of fully ionic species from the decomposition reaction of other solvents. Indeed, an Li electrode in 1,3-dioxolane with LiAsF<sub>6</sub> showed dendrite-free electroplating and high cycling efficiency during cycling.<sup>30</sup> However, in spite of the efficient stabilization of Li electrodes in 1,3-dioxolane with LiAsF<sub>6</sub> electrolyte, the prolonged cycling of Li/Li<sub>x</sub>MnO<sub>2</sub> full cells did not show sufficient cycle performance at a high charging rate.<sup>30</sup>

Considering that detached Li electrodes from dead cells have shown uniform smooth surface morphology and good cycle performance again in a fresh electrolyte, failure of the cells might be caused by the depletion of the electrolyte in the cell, which might be attributed to continuous reactions between the Li and solution components under higher charging conditions. Based on these results, the ideal interphase between Li and the electrolyte might be hermetic, which would completely prevent the Li electrode from contacting the electrolyte. Therefore, ceramic and polymeric protective layers are now being considered as a promising stabilization approach for Li electrodes.<sup>41–44</sup> However, the possibility of severe volume changes of Li during cycling should also be considered to cause mechanical degradation, which will be discussed in detail in the next section.

## 2.2 Prior arts for Li metal anode

As described previously, the nature of the surface layers on Li and the morphology of Li deposits are key factors that determine the cell performance of Li metal batteries. So far, numerous studies have been conducted to resolve the problems of interfacial instability in various ways. In this section, prior

works on Li metal anodes are reviewed in terms of (i) liquid electrolyte, (ii) additives, (iii) polymer-based electrolyte, (iv) Li-surface coating, and (v) electrode and cell configuration.

**2.2.1 Liquid electrolyte: choice of solvent and salt.** The choice of a solvent and Li salt is an important issue, because the nature of the SEI layer and morphology of Li electrodeposits primarily depend on the type of electrolyte solution used. Basically, an organic solvent for an electrolyte solution must be able to dissolve sufficient amounts of Li salt, and thus it usually contains polar groups such as carbonyl (C=O), nitrile (C≡N), sulfonyl (S=O), and ether-linkage (−O−). Various polar organic solvents have been investigated, and carbonate, ether, or ester families have been generally accepted as major solvents for Li batteries.<sup>44</sup> In the early stages of Li battery development, propylene carbonate (PC), a cyclic carbonate, attracted much attention because of its high dielectric constant, static stability with Li metal, and Li electrodeposition capability.<sup>18,45</sup> However, the cycling efficiency of Li in PC-based electrolytes has been poor, which was attributed to PC reduction on newly deposited Li surfaces and dendritic growth of Li.<sup>45,46</sup> Later, another cyclic carbonate, ethylene carbonate (EC), and linear carbonates were investigated, which had a crucial impact on the advancement of Li-ion batteries using Li-intercalation electrode materials. The use of graphitic carbon as an anode in Li-ion batteries was enabled, which brought about successful commercialization.

However, there seem to have been no significant improvements of Li metal anodes regarding the problems of interfacial impedance and the morphology of Li.<sup>47</sup> In the years after the investigation of PC, ether-group solvents came to the fore as another candidate to resolve the issues with Li dendrite growth. Ether solvents such as tetrahydrofuran (THF), 2-methyltetrahydrofuran (2-Me-THF), and diethyl ether (DEE) have low viscosity and high ionic conductivity, and could be used to achieve less dendritic Li deposition.<sup>48</sup> However, prolonged cycling has still led to dendritic Li deposition, and battery performance has not been satisfactory.<sup>49,50</sup> Another problem of ether-based solvents is their limited anodic electrochemical stability.<sup>51</sup> Most ether-based solvents start to oxidize at relatively low potential below 4 V, which restricts their use with 4-V-class cathodes, such as LiCoO<sub>2</sub>, LiNiO<sub>2</sub>, and LiMn<sub>2</sub>O<sub>4</sub>. However, a recent revisiting of the Li-S battery system has aroused new interest in ether solvents, since the charging cut-off potential of an S cathode is below 3 V. The dissolved polysulfide anions are stable in ether-based solvents, but not in carbonate-based ones.<sup>52</sup>

There are some functional solvents that can improve the performance of Li metal anodes. For example, Yamaki *et al.*<sup>53</sup> investigated a series of partially fluorinated esters as a sole solvent. Compared with the non-fluorinated esters, the partially fluorinated esters showed enhanced cycling performance and thermal stability, which may have been brought about by a robust SEI layer on the Li metal anode. Zhang and Angell<sup>54</sup> studied boric acid esters of glycol (BEG) as a possible co-solvent for Li-metal-based batteries. Because of the great propensity for dissolving Li salts, stabilizing Li metal against corrosion, and increasing stability against anodic decomposition, Li metal could remain shiny upon prolonged immersion, even at

elevated temperature. Excellent cycling performance was observed in an Li–LiMn<sub>2</sub>O<sub>4</sub> system. A tetramethylene sulfone, known as sulfolane, was suggested as another possible solvent for Li-metal-based batteries. Matsuda *et al.*<sup>55</sup> studied sulfolane as a co-solvent combined with ether-based solvents. They found that the composition of LiPF<sub>6</sub> in sulfolane/dimethoxyethane enhanced the Li cycling efficiency, probably due to the stabilized interphase at the Li metal anode.

The Li salts for an electrolyte solution are not as diverse as the solvent material. The major salts which have been qualified for Li batteries include lithium perchlorate (LiClO<sub>4</sub>), lithium hexafluoroarsenate (LiAsF<sub>6</sub>), lithium hexafluorophosphate (LiPF<sub>6</sub>), lithium tetrafluoroborate (LiBF<sub>4</sub>), lithium trifluoromethanesulfonate (LiOSO<sub>2</sub>CF<sub>3</sub>), and lithium bis(trifluoromethane-sulfonyl)imide (LiN(SO<sub>2</sub>CF<sub>3</sub>)<sub>2</sub>, LiTFSI). Unfortunately, none of the Li salts could completely resolve the problem of Li dendrite formation, but the static interfacial impedance and the degree of Li dendrite formation have differed depending on the kind of Li salt used. It was reported that the chemical composition of the SEI layer on Li metal was not changed significantly when LiClO<sub>4</sub> salt was used.<sup>47</sup> In addition to organic compounds formed from organic solvents, the weak formation of LiCl was observed, which was possibly due to the chemical reaction between ClO<sub>4</sub><sup>−</sup> anions and the native film and/or fresh Li metal. The LiClO<sub>4</sub> is likely to have provided lower SEI impedance compared with LiPF<sub>6</sub> or LiBF<sub>4</sub>. However, it could not suppress the formation of Li dendrites. Also, the high oxidation state of chlorine in perchlorate has been problematic under certain conditions, such as high temperature and high current charge.<sup>56</sup> This salt has been regarded as impractical in Li battery applications. LiAsF<sub>6</sub> was once widely investigated combined with ether solvents to suppress the formation of Li dendrites. Li metal anodes in electrolytes containing LiAsF<sub>6</sub> showed dendrite-suppressed electrodeposition and high cycling efficiency.<sup>30</sup> It is known that LiAsF<sub>6</sub> reduces at around 1.15 V (vs. Li/Li<sup>+</sup>),<sup>30,57</sup> and produces LiF and Li<sub>x</sub>AsF<sub>y</sub> at the surface layers, which probably has a positive effect on the interfacial stability of the Li metal anode. However, the morphological behavior of Li has been inconsistent between studies,<sup>30,33,47,57</sup> and safety concerns regarding the toxicity of the As element prohibits the use in any commercialized batteries.

LiPF<sub>6</sub> is now generally accepted as the most suitable Li-salt, because of its well-balanced properties for various requirements as an electrolyte.<sup>44</sup> This salt has successfully been employed in commercialized Li-ion batteries. However, since LiPF<sub>6</sub> is hygroscopic and chemically/thermally unstable, it can produce HF as a result of the decomposition of PF<sub>6</sub><sup>−</sup> through chemical reaction with trace water in an electrolyte solution. There is a general consensus that the generated HF can attack oxide-based cathode material, resulting in capacity loss during cycling in Li batteries.<sup>58</sup> However, the HF can promote the interfacial stability of the Li metal anode. Takehara<sup>20</sup> investigated the effect of LiPF<sub>6</sub> salt on SEI layers and the morphology of Li electrodeposits, and identified the formation of a thin LiF layer with good protective ability, which led to smooth Li deposits and improved cycling efficiency. Later, the effect of HF on Li metal was also presented by directly adding a small

amount of HF to an electrolyte,<sup>59</sup> which was effective for the suppression of Li dendrite formation. LiBF<sub>4</sub> was also studied as a possible Li salt for controlling the interfacial properties of Li metal anodes.<sup>60</sup> Similar SEI properties to those of LiPF<sub>6</sub> were demonstrated, which was expected to improve the performance of the Li metal anode. However, its small dissociation constant, which is associated with relatively low ionic conductivity, hinders its wide use as a main solute in electrolyte solutions. LiOSO<sub>2</sub>CF<sub>3</sub> and LiTFSI are other promising Li salts, and have high dissociation constants, high oxidation and temperature stability, nontoxicity, and insensitivity to moisture. Unfortunately, they seem to have no beneficial effects on Li metal anodes with respect to the interfacial and morphological properties of Li deposits.<sup>61</sup> However, another Li imide salt, lithium bis(perfluoroethylsulfonylimide) (LiN(C<sub>2</sub>F<sub>5</sub>SO<sub>2</sub>)<sub>2</sub>, LiBETI), was found to produce very uniform, thin, and stable SEI layers on Li metal anodes.<sup>61</sup> The SEI layer formed in an LiBETI–PC system was hemispherical, and the composition of the film consisted mainly of LiF, which is similar to that in LiPF<sub>6</sub>–PC systems. The LiBETI–PC system provided a compact and smooth surface morphology during Li deposition–dissolution cycles.

Recently, ionic liquids have attracted much attention as a new class of electrolytes for Li-based batteries. Ionic liquids are less volatile and typically non-flammable, which can enhance the safety of Li batteries. Several studies on the compatibility of ionic liquids with Li metal have been reported,<sup>62–67</sup> which suggested that some ionic liquids could suppress the formation of Li dendrites and enhance the cycling performance. It is generally considered that 1-alkyl-3-methylimidazolium cations are not quite stable enough to be inert toward Li,<sup>62</sup> which is probably due to the acidity of the proton in the cation ring. However, the substitution of a proton moiety or a different type of anion could change the behavior.<sup>63</sup> Pyrrolidinium-based ionic liquids were identified to show a remarkable increase in reductive stability compared with those based on imidazolium.<sup>62,64</sup> Highly reversible deposition–dissolution of Li metal was achieved, and the formation of Li dendrites was suppressed. For example, Howlett *et al.*<sup>64</sup> investigated *N*-methyl, *N*-alkyl pyrrolidinium bis(trifluoromethanesulfonyl)amide (P<sub>1X</sub>(Tf)<sub>2</sub>N, X = 3,4) for use in Li metal batteries. Uniform Li deposits over many cycles could be achieved at moderate current densities, resulting in cycling efficiency of more than 99%. It was suggested that stable P<sub>1X</sub><sup>+</sup> cations at a negative potential and SEI layers formed from the anions played an important role in the enhancement. For further advancement of ionic liquids for Li metal, the need for a systematic study to find a highly fluidic ionic liquid with sufficient stability against Li metal and dendrite-free Li deposits remains.

**2.2.2 Additives.** The use of low-concentration additives is an effective and efficient method for controlling the Li metal interface. These additives can modify the physical and chemical properties of the SEI layer, and control the current distribution during Li electrodeposition. The mechanism of the additive function can be classified roughly into three categories: (i) reaction with the Li metal and/or native Li surface film producing uniform and dense SEI layers, (ii) non-reactive

additives controlling the current distribution or reducing Li reactivity with bulk electrolyte solution, and (iii) *in situ* Li-alloy formation affecting electrodeposited Li morphology. Various types of additives have been explored so far, including inorganic compounds,<sup>8,20,22,34,59,68–74</sup> organic compounds such as surfactants,<sup>18,53,75–84</sup> and gaseous compounds.<sup>18,68,85</sup> These additives are summarized in Table 2 with their function. Some noteworthy studies are described.

Hydrogen fluoride (HF) was proposed by Kanamura and Takehara as an additive to modify the SEI layers.<sup>20,22,34,59</sup> A small amount of HF added to an organic liquid electrolyte caused an acid-base reaction with the native Li surface layers, which were mainly composed of  $\text{Li}_2\text{O}$ ,  $\text{LiOH}$ , and  $\text{Li}_2\text{CO}_3$ , and finally produced an  $\text{LiF-Li}_2\text{O}$  bilayer. The  $\text{LiF}$ -containing SEI showed a less-defective, uniform, and dense layer, and induced an even current distribution during Li deposition and dissolution. Accordingly, smooth hemispherical Li deposits called *blue lithium* were provided (Fig. 5), indicating the uniformity of the Li deposits, which consequently improved the cycling efficiency of the Li metal anode. These effects of HF on the Li metal anode could be observed in an electrolyte solution containing  $\text{LiPF}_6$ , where the  $\text{LiPF}_6$  decomposes with trace  $\text{H}_2\text{O}$  in the electrolyte and generates HF,<sup>22</sup> as well as in the other active fluorine-containing additives, such as  $(\text{C}_2\text{H}_5)_4\text{NF}(\text{HF})_4$ <sup>75</sup> and fluorinated ester.<sup>53</sup>

To suppress dendritic Li electrodeposits, non-reactive additives have also been investigated. The adsorption of the non-reactive additive at the interface inhibits the reaction between Li metal and electrolyte solution, which maintains the SEI layer as thin and chemically stable by retarding the growth of an undesirable highly resistive SEI layer. The additive can also be expected to affect the mechanism of electrodeposition. The adsorbed additive could promote the two-dimensional nucleation and growth of electrodeposited metal.<sup>86</sup> The additive may also act as a levelling agent leading to smooth electrodeposits. The diffusion- or ohmic-controlled current distribution is one of the major causes of uneven or dendritic electrodeposits.<sup>86</sup> The adsorbed additive can alter the diffusion- or ohmic-controlled

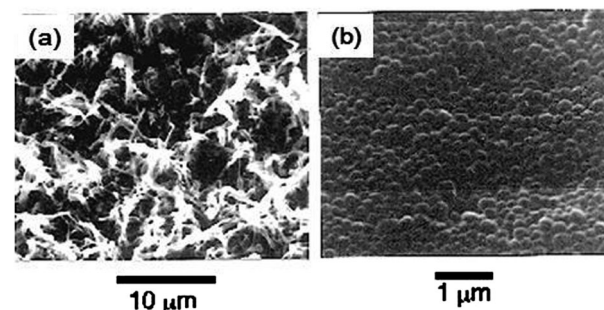


**Fig. 5** SEM images of Li electrodeposited on a Ni substrate in 1.0 M  $\text{dm}^{-3}$   $\text{LiClO}_4/\text{EC} + \text{DME}$  (a) without and (b) with HF (The American Chemical Society, reprinted with permission).<sup>59</sup>

current distribution, which is dominant in Li metal interface systems, to the activation-controlled current distribution<sup>87</sup> in the irregular interface situation of Li metal anodes. Therefore, the use of additives to achieve a uniform current distribution may be one approach to solving the problems of dendritic Li deposition. Naoi *et al.*<sup>82</sup> studied the effect of polyether-type surfactants (polyethyleneglycol dimethyl ether and a copolymer of dimethylsilicone and propylene oxide). The adsorption of the surfactants provided a more uniform current distribution, which resulted in a significant suppression of the localized Li deposition. The surfactants also stabilized the surface film, which showed little change in resistance for several days and throughout long cycling. Non-reactive and non-polar substances such as decalin<sup>80</sup> and benzene<sup>77</sup> compounds were also reported as possible additives for Li metal anodes. They are accumulated, or physically adsorbed, at the Li interface, and probably inhibit the reaction of Li with electrolyte solution, and limit the growth of the undesirable surface film. It provided the Li surface with a more uniform activity, which results in a more uniform and smoother Li deposit.

Another type of additive for suppressing dendritic Li deposits is based on Li-alloying reaction (or co-deposition) with another

**Table 2** Various additives in an electrolyte solution for the Li metal anode

Additives	Function and effect	Ref.
Inorganic HF, polysulfides $\text{S}_x^{2-}$ , $\text{POCl}_3$ $\text{Mg}(\text{ClO}_4)_2$ , $\text{AlI}_3$ , $\text{SnI}_2$ , $\text{MgI}_2$ , $\text{LiI}$ , $\text{AlCl}_3$ , $\text{Na}(\text{CF}_3\text{SO}_2)_2\text{N}$ $\text{CsPF}_6$ , $\text{RbPF}_6$	SEI modification, suppressed dendrite Li-alloy interphase, suppressed dendrite Adsorption of non-reactive metal cation, dendrite-free	20, 22, 34, 59, 68, 69 8, 70–74 88
Organic $(\text{C}_2\text{H}_5)_4\text{NF}(\text{HF})_4$ , fluorinated ester, vinylene carbonate, 2-methylfuran, 2-methylthiophene, nitromethane, fluoroethylene carbonate, <i>N</i> -methyl- <i>N</i> -(butyl sulfonate) pyrrolidinium (zwitterion) Benzene, decalin, tetraalkylammonium chlorides poly(ethylene glycol) dimethyl ether, dimethyl silicone/propylene oxide copolymer, poly-ether modified siloxanes, tetraethylammonium perfluorooctanesulfonate	Reactive additives, SEI modification, suppressed dendrite Adsorption, less reactive interface, suppressed dendrite	53, 75, 76 18, 77, 78 79 77, 80, 81 82 82 83 84
Gaseous $\text{CO}_2$ , $\text{SO}_2$ , $\text{N}_2\text{O}$	SEI modification, granular deposit	18, 68, 85

metal such as Na,<sup>74</sup> Mg,<sup>70,72</sup> Al,<sup>71</sup> and Sn<sup>71</sup> from an electrolyte solution containing a small amount of metal salt additive. It was postulated that when metal ions are electrochemically reduced and deposited on the Li metal surface, they produce a thin Li-alloy surface layer, which could ease the irregularity of the Li interface. The improved uniformity of the interface by the Li-alloy formation provides a relatively even current distribution and suppresses dendritic Li deposits, and finally increases the Li cycling efficiency.

Contrary to the Li-alloying mechanism of the above additives, a new concept of electrostatic shield mechanism by another metal cation has been reported by Ding *et al.*<sup>88</sup> The controlled small addition of Cs<sup>+</sup> or Rb<sup>+</sup> cations led to alteration in their effective reduction potential below the standard reduction potential of Li ions. The adsorption of the metal cations resulted in the formation of a positively charged electrostatic shield around the initial growth tip of the Li deposit without reducing the additives, which forced further uniform and dendrite-free deposition of Li. Although this strategy realized remarkably smooth Li deposits, the still low cycling efficiency of the Li anode (76.5%, *cf.* 76.6% for the additive-free electrolyte) should be resolved. Also, the morphology of Li deposits at a high charging rate (over 1 mA cm<sup>-2</sup>) needs to be investigated for application in practical rechargeable Li metal batteries.

**2.2.3 Polymer electrolyte.** As discussed previously, the dendrite formation of Li during charging lowers the cycling efficiency and eventually incurs internal short-circuit, leading to an explosion of the battery in the worst case. Compared with a liquid electrolyte, a continuous or non-porous polymeric electrolyte can mitigate the aforementioned problems to a lesser extent. Also, the polymer-based electrolyte is expected to be less reactive to Li metal due to the solid-like nature and much lower liquid content, which alleviates the formation of a highly resistive passivation layer and/or the self-discharge of Li metal. However, the phenomenon of Li dendrite formation still exists, and the interfacial resistance by the SEI formation should be further improved for practical battery applications.

For a Li-ion conductive polymer electrolyte, several polymer host materials such as poly(ethylene oxide) (PEO), poly(propylene oxide) (PPO), poly(acrylonitrile) (PAN), poly(methyl methacrylate) (PMMA), poly(vinylidene fluoride) (PVdF), poly(vinylidene fluoridehexafluoropropylene) (PVdF-HFP), polysiloxanes (PS), and polyphosphazenes (PPhz) were investigated.<sup>89,90</sup> Of these, PEO and PPO have been widely studied because of the more stable complexation with Li salts and higher ionic conductivity. PS and PPhz based polymers were also paid attention due to their high flexibility and conductivity, and enhanced interfacial stability with Li.<sup>91,92</sup> To further improve the properties of polymer electrolytes, various materials such as ionic liquids<sup>93–97</sup> and/or inorganic fillers<sup>95,98–100</sup> were incorporated into the host polymers to produce the composite polymer electrolytes (CPE), which exhibited positive effects on the Li metal electrode. In addition, an organic–inorganic hybrid electrolyte concept was also introduced where the inorganic material strengthened the dimensional stability of electrolytes, maintaining high ionic conductivity.<sup>101,102</sup>

Imanishi *et al.*<sup>93–95</sup> reported on the behavior of Li dendrite formation in composite polymer electrolytes with an ionic liquid added, such as poly(ethylene oxide) (PEO)-lithium bis(trifluoromethanesulfonyl)imide (LiTFSI) with *N*-methyl-*N*-propylpiperidinium-bis(fluorosulfonyl)imide (PP13FSI) added. The addition of the ionic liquid, which has been known for its good electrochemical and thermal stability as an electrolyte in Li-metal based cells, resulted in higher ionic-conductivity and lower interfacial resistance than that achieved with the normal PEO–LiTFSI polymer electrolyte. Consequently, the retardation of Li dendrite growth led by the enhanced interfacial stability could be achieved, which was directly confirmed using an *in situ* optical visualization cell (Fig. 6).

Another approach is to add a nano-sized ceramic filler powder to a polymer electrolyte. The original reasoning behind the incorporation of a ceramic filler was to enhance the mechanical stability of the polymer electrolyte.<sup>103</sup> However, the addition also improved the ionic conductivity and Li/electrolyte interfacial compatibility.<sup>90,94</sup> The principle mechanism for the enhanced ionic conductivity has been known as the local formation of the amorphous phase of the polymer around each filler particle, which provides a preferential Li ion pathway.<sup>99,104</sup> However, the role of the filler in promoting the Li ion transport still remains to be addressed clearly. As mentioned, the polymer electrolyte with filler added also provided better Li/electrolyte interfacial compatibility, which strongly depended on the particle size<sup>8</sup> and/or the nature<sup>105</sup> of the filler. The improved interfacial compatibility with the homogeneously distributed filler particles at the interface probably (i) reduced the reactivity of Li with the electrolyte, (ii) supported stiffness and compressibility to suppress Li dendrite growth, and (iii) induced an even current distribution during charging and discharging. These effects would result in less cell impedance and improved cycling performance. For instance, Imanishi's group further improved the performance of

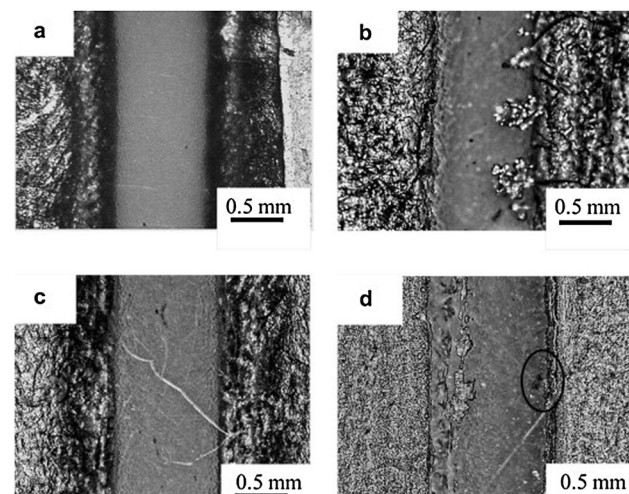


**Fig. 6** Dendrite growth of Li in the Li/PEO<sub>18</sub>LiTFSI/Li and Li/PEO<sub>18</sub>LiTFSI-1.44PP13FSI/Li cells at 0.1 mA cm<sup>-2</sup> and at 60 °C. (a) Li/PEO<sub>18</sub>LiTFSI/Li for *t* = 0 h, (b) Li/PEO<sub>18</sub>LiTFSI/Li for *t* = 210 h, (c) Li/PEO<sub>18</sub>LiTFSI-1.44PP13FSI/Li for *t* = 0 h, and (d) Li/PEO<sub>18</sub>LiTFSI-1.44PP13FSI/Li for *t* = 256 h (Science Direct, reprinted with permission).<sup>94</sup>

Li metal in a composite polymer of PEO–LiTFSI and PP13TFSI by adding nano-SiO<sub>2</sub> powder.<sup>95</sup> They identified higher ionic conductivity, less interfacial impedance, and the further inhibition of dendrite growth of Li, and suggested the composite as an electrolyte for all solid-state lithium metal batteries, or as a buffer layer between Li metal and the NASICON-type inorganic solid electrolyte for Li–air batteries.

From these beneficial effects of nanosized inorganic particles on the polymer electrolyte, one can reasonably expect that the composite polymer electrolytes with layered silicate<sup>106–108</sup> and ordered mesoporous inorganic materials<sup>109,110</sup> would be helpful to improve the dimensional stability and interfacial compatibility of the polymer electrolyte with Li metal. In particular, it is expected that nanocomposite polymer electrolytes with a more rigid inorganic framework might show enhanced electrochemical performances against severe volume and shape changes of the Li electrode during cycling.

**2.2.4 Surface coating.** Another approach to stabilize the SEI layer and suppress dendritic Li deposits involves pre-coating the Li metal surface by a relevant substance. A pre-coating substance should be structurally uniform and thin for an even current distribution, and have other properties such as small impedance, chemical stability against the electrolyte, interface-forming ability with good contact, and mechanical durability. Several relevant studies have been conducted on coatings for possible applications, such as silane-based coatings,<sup>111–114</sup> polymer-based coatings,<sup>115–118</sup> and inorganic Li-ion conductive coatings such as Li<sub>3</sub>N<sup>119</sup> and Li phosphorus oxynitride (LiPON).<sup>120</sup> Dunn<sup>111</sup> and Vaughey<sup>113,114</sup> reported on chlorosilane pre-treatment of the Li metal surface for improving the performance of Li metal anodes. The layer formed by the self-terminating reaction between the chloride substituent and a hydroxyl-terminated layer on the Li metal led to a low initial interfacial impedance, and retarded the corrosion of the Li metal anode. However, the cohesiveness of the coatings was gradually disrupted during cycling, and further development was needed to obtain satisfactory cycle performance.

An ultraviolet-curable semi-interpenetrating polymer network (IPN) was reported as a polymer-based protective layer.<sup>118</sup> Pre-coating of the semi-IPN delivered a stabilized interfacial impedance and less dendritic Li deposit than that of the untreated Li anode, leading to improved cycle performance. The result depended on the condition of the cross-linking agent. The reason was not clear, but the uniformity with fewer defects and good contact between coatings and the Li metal may play an important role in the improved performance.

**2.2.5 Electrode and cell configuration.** It has consistently been identified in many studies on Li metal anodes that the morphology of the Li deposit critically depends on the current density, in that as the current density increases, the Li deposit exhibits dendritic formation.<sup>37,121–124</sup> Rosso *et al.*<sup>123</sup> have established the relationship between the onset time of dendritic growth of Li and the current densities based on experimental results using an Li/polymer cell. The onset time was delayed as the current density decreased. Monroe and Newman<sup>124</sup> developed a model to predict the tip growth rate of Li dendrites, and concluded that it would be

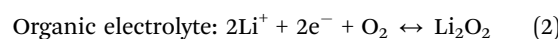
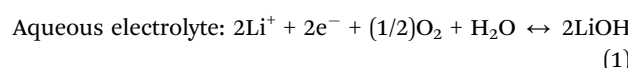
decreased when the current density was reduced. The use of Li metal powder instead of Li foil is one technique to lower the effective current density at the Li anode.<sup>122,125</sup> The Li metal powder provides higher interfacial area than Li foil, and reduces the effective current density at the anode, resulting in suppressed dendritic formation of the Li deposits and enhanced cycle performance. Recently, the use of a three-dimensional current collector with a high surface area has also been investigated to suppress dendritic Li deposition by lowering the practical current density.<sup>9,126,127</sup> A detailed discussion is presented in Section 2.3.3.

Apart from material and electrochemistry approaches, external physical factors such as cell-stacking pressure<sup>128,129</sup> and temperature<sup>130</sup> can also influence the morphology of Li deposits. Li metal anodes cycled under a certain pressure showed a densely-packed Li deposit layer, where the possibly isolated Li still maintained electrical contact. In an all-solid-state battery, the cell-stacking pressure was one of the factors that determined the cell performance.<sup>128</sup> Since the conductivity of the inorganic solid electrolyte was comparable to that of a liquid electrolyte system, the interfacial resistance was a more significant problem in this system. The repeated dissolution and deposition of Li metal can lead to failure of interface formation due to the generation of voids or a resistive surface layer, which results in the degradation of the cell performance. However, the interfacial resistance can be reduced simply by imposing high pressure, which promotes intimate mechanical contact at the interface.

### 2.3 Recent progress in Li metal anodes

Recently, Li–air(O<sub>2</sub>) and Li–S batteries have attracted much attention due to their high energy density compared to current Li-ion batteries. The high energy density of both Li batteries basically originates from the use of metallic Li as a negative electrode, as well as the high-capacity positive electrodes. To realize commercial Li–air and Li–S batteries, the technical problems associated with the Li metal anode must be solved. In this section, specific issues of Li metal electrodes in Li–air and Li–S batteries are summarized, and the recent progress in Li metal electrodes is reviewed.

**2.3.1 Issues in Li–air batteries.** Besides suppressing the Li dendrite formation, a major challenge in Li–air batteries is to protect the surface of the Li metal from exposure to water and gases such as oxygen and CO<sub>2</sub>, which results in electrode degradation and safety problems.<sup>5,131–133</sup> In aqueous Li–air systems, the Li metal should be separated from the aqueous electrolyte solutions by Li<sup>+</sup>-conducting solid membrane materials, as shown in Fig. 7, because metallic Li is very reactive with water. For non-aqueous electrolyte batteries, undesirable reactions of the Li electrodes with the gas molecules in air or gas contaminants in the non-aqueous electrolytes need to be prevented. The overall reaction chemistries involved in each electrolyte can be expressed as<sup>131–133</sup>



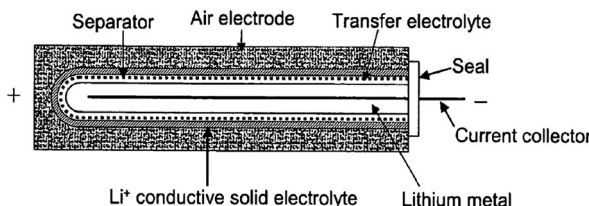


**Fig. 7** Schematic of a cylindrical Li-air cell employing a glass ceramic protective layer.<sup>142</sup>

**2.3.2 Issues in Li-S batteries.** The Li metal anodes of Li-S batteries have different issues from other Li batteries.<sup>134–137</sup> During the first discharge process, elemental S is reduced to form soluble Li polysulfides, followed by the final insoluble products such as Li<sub>2</sub>S. In the later stages of the subsequent charge process, the higher-order polysulfides are generated at the S cathode, and diffuse through the separator into the Li electrode to form the lower-order polysulfides by a parasitic reaction with the Li. These species diffuse back to the S electrode to produce the higher-order polysulfide again. The shuttle process occurs repeatedly, which leads to a decrease of the active mass utilization and the Coulombic efficiency of Li-S cells. The overall reaction chemistry is<sup>134</sup>



**2.3.3 Recent progress.** Other than dendrite formation, recent research efforts on Li metal electrodes have mainly been devoted to protecting the Li metal surface using various Li-ion conducting materials to prevent undesirable access to gas molecules and Li polysulfides. The application of a protective layer coating for Li metal electrodes has been a typical method for blocking these species, as well as for resisting the formation of dendrites or mossy deposits upon cycling.<sup>138,139</sup>

Glass ceramic materials such as Li super-ionic conductor (LISICON) are commonly used as protective layers and SEIs. A representative material is Li<sub>1+x</sub>Al<sub>x</sub>Ti<sub>2-x</sub>P<sub>3-y</sub>Si<sub>y</sub>O<sub>12</sub> (LATP), which shows a very high Li-ion conductivity of  $\sim 10^{-3}$  S cm<sup>-1</sup> at room temperature.<sup>140,141</sup> When this material directly contacts Li metal, LISICON is expected to be unstable. Therefore, to avoid undesirable reactions between the two materials, a secondary protection layer is needed. Recently, Visco *et al.* of the PolyPlus Battery Company demonstrated a multi-layered Li electrode consisting of Li metal, a gel electrolyte (or a non-aqueous liquid electrolyte with a separator), and an Li-ion conducting glass ceramic layer, as shown in Fig. 7.<sup>142</sup> In this protective architecture, a gel polymer electrolyte was placed between the Li metal and an LATP glass ceramic layer in order to block the direct contact.

The secondary layer should also have a high Li-ion conductivity, and should be stable when in contact with Li metal. Several materials have been suggested for their high ionic conductivity and stability with Li, such as Li<sub>3</sub>N, Cu<sub>3</sub>N, LiPON, and polymer electrolytes.<sup>133</sup> A research group at Mie University has actively worked on this topic.<sup>143–146</sup> Imanishi *et al.* reported that LiPON was effective as the buffer layer to prevent the

irreversible reaction of LATP with Li metal, although the interfacial resistance required reduction for low-temperature operation.<sup>143,144</sup> Zhang *et al.* also investigated a polymer material of poly(ethylene oxide) (PEO) with LiN(SO<sub>2</sub>CF<sub>3</sub>)<sub>2</sub> (LiTFSI) salt as an interlayer,<sup>145,146</sup> which had suitable performance. When nanosized BaTiO<sub>3</sub> was finely dispersed in the PEO-based polymer, the interfacial resistance with Li metal was greatly reduced.<sup>146</sup> An aqueous Li-air prototype cell was demonstrated using this PEO-based interlayer and the LATP glass ceramic protective layer (Fig. 8).<sup>147</sup> The cell showed an energy density of 779 W h kg<sup>-1</sup>, which is about two times larger than that of a conventional graphite/LiCoO<sub>2</sub> cell. Although the multi-layered glass ceramic protective architecture appears promising, problems exist. The layer must be prepared as a thin, flat film, and the development of a large-scale production process is required for practical applications. Moreover, the interfacial resistance between the interlayer and Li metal is generally high, and it must be minimized.

A different approach to suppress Li dendrite formation is using three-dimensional (3D) current collectors.<sup>9,126,127</sup> By increasing the surface area of current collectors through the use of a 3D architecture, the current density for Li deposition and dissolution can be significantly reduced, which results in dendrite control during Li cycling. Wang *et al.* investigated the effect of the Ni foam substrate on Li electrodes.<sup>9</sup> Li was electrodeposited on the Ni foam, which had a surface area seven times larger than that of Li foil. The interfacial resistance of the foamed Li anode was lower than that of Li foil, and improved cycling performance was obtained by prohibiting the formation of Li dendrites. This can be explained by the decreased effective current density caused by the increased surface area of the foam structure. Spatially heterogeneous carbon-fiber paper was recently introduced as a current collector by Stucky *et al.*<sup>127</sup> Dendrite-free Li metal was observed using 3D current collectors decorated with SiO<sub>2</sub> or SiC, even after prolonged cycling. The electrode maintained a constant volume upon deposition, which was afforded by the large porous volume of the current collector. The scaffold-like structure of the carbon paper prevented the disintegration of deposited Li.

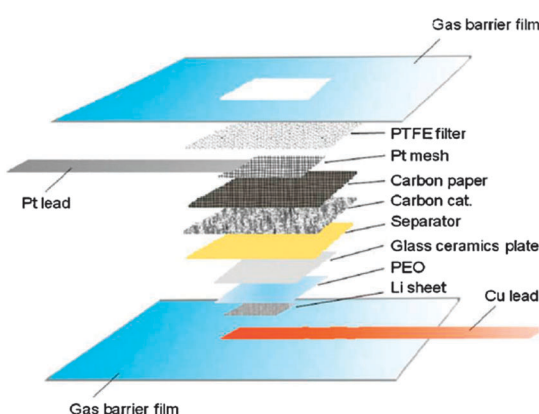


**Fig. 8** Schematic of the proposed Li-air system (The Royal Society of Chemistry, reprinted with permission).<sup>147</sup>

Zhamu *et al.* reported the use of graphene sheets as a current collector.<sup>126</sup> Graphene material is well known to have a very high surface area that significantly reduces the effective electrode current density. Fig. 9 shows a schematic illustration of the concept. Li–vanadium oxide full cells were tested to investigate the effect of the graphene sheets. After 500 cycles, the cell capacity was well maintained without Li dendrite formation, which could be ascribed to the decreased current distribution by graphene.

Another method for Li–S batteries involves LiNO<sub>3</sub> addition to the electrolyte solution.<sup>148–153</sup> Recently, Milkhaylik of Sion Power Corporation patented an additive that includes an N–O bond.<sup>148,149</sup> It was reported that the use of LiNO<sub>3</sub> as an additive prevented the detrimental shuttle process in Li–S batteries. Aurbach *et al.* investigated the effect of LiNO<sub>3</sub> using electrochemical and spectroscopic analyses.<sup>150</sup> When LiNO<sub>3</sub> was added to the electrolyte solution in Li–S cells, the reversible capacities were increased. In FT-IR and XPS analyses, it was found that the presence of LiNO<sub>3</sub> in the solution had a pronounced impact on the surface chemistry of the Li electrode. Li<sub>x</sub>NO<sub>y</sub> surface species and various Li<sub>x</sub>SO<sub>y</sub> surface moieties were formed by the reduction of LiNO<sub>3</sub> and the oxidation of sulfur species, respectively. This phenomenon prevented the full charging of the sulfur electrodes in the Li–S cells. Enhancement of the passivation layer on the Li metal diminished the possibility of reactions of the polysulfide species with active Li metal, which resulted in an improvement of the electrochemical properties of Li–S cells. Liang *et al.* prepared an electrolyte with LiNO<sub>3</sub> added, and tested the electrochemical properties of Li–S cells.<sup>151</sup> Compared to a cell without LiNO<sub>3</sub>, the Li–S cell containing the additive exhibited highly improved cycling efficiency and stability up to 50 cycles, which could be attributed to the protective SEI layer formation induced by LiNO<sub>3</sub>.

Recently, several groups demonstrated the Li metal free Li–S battery system by replacing the Li metal anode with a pre-lithiated Si electrode.<sup>154–157</sup> Since the activity of Li in the Li–Si

alloy phase is less than unity, technical problems related with the use of metallic Li can be mitigated, thus showing a promising electrochemical behavior. However, Li-alloy anode materials also have some problems such as mechanical stability and poor cycle performance associated with huge volume changes of Si during cycling.<sup>2</sup> It should be noted that a reliable operation process with the additional facility for prelithiation of Li-alloying electrodes might increase the production cost of Li-metal free Li–S battery systems.

An analytical investigation of the formation of Li dendrites and mossy Li was recently performed. Grey *et al.* reported time-resolved quantitative information about the nature of electrochemically deposited metallic Li using *in situ* NMR spectroscopy in conjunction with electrochemical cycling.<sup>158</sup> They demonstrated that it was possible to quantify the amount of dendritic/mossy Li by analyzing the change in the signal intensity of the Li metal during cycling. Recently, imaging techniques that enable non-invasive visualization and characterization of the changes occurring in electrodes and electrolytes in batteries were introduced.<sup>159</sup> The location of the Li-metal deposits could be determined during Li cycling by using magnetic resonance imaging (MRI) technology. Fig. 10 shows two-dimensional <sup>7</sup>Li MRI images taken before and after cell charging. The conditions related to the formation of dendritic/mossy Li could be explored and quantified using this imaging technique. The approach could also be extended to investigate the microstructure of other electrode materials.

Efforts to modify the separators in contact with Li metal have been reported.<sup>160,161</sup> Ryou *et al.* demonstrated that improved cycle behavior of Li metal electrodes could be obtained by using polydopamine-treated polyethylene (PE) separators.<sup>160</sup> The polydopamine treatment could make the PE surface hydrophilic, and thus increase the uptake amount of the liquid electrolyte. The enhanced electrolyte uptake could lead to well-distributed Li-ionic flux on the electrode surface, which might lessen the Li dendrite growth. Another suggested reason for the improvement was the strong mussel-inspired catecholic adhesion of polydopamine onto the Li surface,

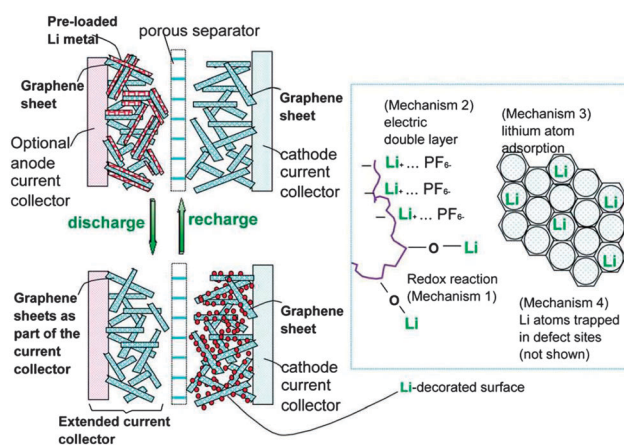


Fig. 9 Structure of a Li-graphene cell before and after the first discharge and plausible mechanisms with which graphene surfaces can capture Li ions at the cathode (The Royal Society of Chemistry, reprinted with permission).<sup>126</sup>

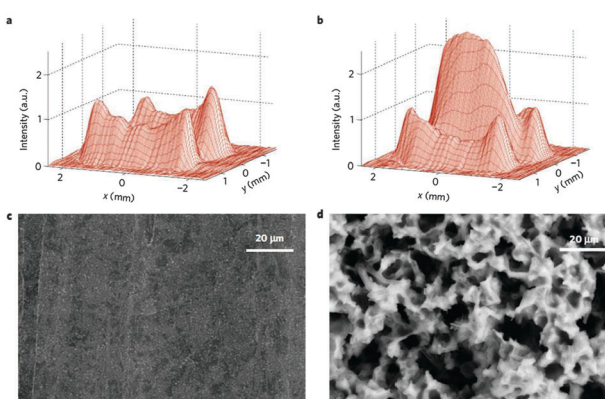


Fig. 10 <sup>7</sup>Li magnetic resonance and SEM images of Li microstructure formation in a Li bag cell. <sup>7</sup>Li two-dimensional MRI x–y images (a) in the pristine state and (b) after charging. SEM images (c) in the pristine state and (d) after charging (Nature Publishing Group, reprinted with permission).<sup>159</sup>

which had a positive influence on the morphological changes of the Li metal. A polypropylene (PP) separator grafted by methyl methacrylate (MMA) was prepared by Ju *et al.*<sup>161</sup> It was found that the MMA functional groups could improve the stability of the interface between the liquid electrolyte and the Li metal anode. A membrane with a three-dimensional ordered macroporous (3DOM) structure was proposed by Kanamura *et al.*<sup>162</sup> The Li electrode with the 3DOM separator exhibited enhanced cycling stability without Li dendrite formation, which could be attributed to the homogeneous current distribution by the 3DOM separator.

### 3. Metallic magnesium (Mg) electrode

Mg is the fourth most common element on earth (next to iron, oxygen, and silicon), and it is the third most abundant element dissolved in seawater. Also, Mg is a light and relatively cheap metal whose reduction potential is  $-2.356\text{ V}$  (vs. SHE), and its potential capacity is *ca.*  $2200\text{ mA h g}^{-1}$  ( $3833\text{ mA h cm}^{-3}$ ). Additionally, Mg is much safer to use and handle than Li, and its compounds are non-toxic. By virtue of the various advantages of Mg, it is a natural candidate as an anode material in high-energy-density battery systems. Several rechargeable Mg-based battery systems have been reported.<sup>163–169</sup> Despite its advantages, the application of Mg to rechargeable batteries has had several problems: (i) the relative difficulty of diffusion of a  $\text{Mg}^{2+}$  ion in a solid-state electrode compared to a monovalent Li ion, (ii) the growth of a passivating surface film<sup>170</sup> composed of  $\text{MgO}$ ,  $\text{MgCO}_3$ , and  $\text{Mg(OH)}_2$ , which cannot transport the  $\text{Mg}^{2+}$  ions, (iii) a narrow electrochemical window of electrolytes for Mg-ion dissolution-deposition, and (iv) relatively low specific energy of the Mg-ion battery.

In spite of the problems associated with Mg metal electrodes, the first rechargeable prototype Mg battery system was reported in 2000 by Aurbach's group, which was composed of an Mg foil anode, an  $\text{Mg}_x\text{Mo}_3\text{S}_4$  cathode, and an organic electrolyte based on Mg organohaloaluminate salts in THF (Fig. 11).<sup>164</sup> Since then, much effort has been made to realize high-performance next-generation rechargeable Mg batteries. Most research on

**Table 3** Comparison of electrochemical performances of various positive electrodes for rechargeable Mg batteries.<sup>164,169,171–176</sup>

Cathode materials	Mg-insertion/ formula unit	Specific capacity ( $\text{mA h g}^{-1}$ )	Potential (V)
$\text{Mo}_3\text{S}_4$ <sup>164</sup>	1	122	1–1.5 <sup>a</sup>
$\text{MoS}_6\text{Se}_2$ <sup>169</sup>	2	102	0.5–2 <sup>a</sup>
$\text{MoS}_2$ <sup>171</sup>	0.66	170	1.5–2.5 <sup>a</sup>
[Hol/AB] $\text{MnO}_2$ <sup>172</sup>	0.09–0.39	85–209	1.85–4.75 <sup>b</sup>
$\text{TiS}_2$ nanotubes <sup>173</sup>	0.49	236	0.5–2.0 <sup>a</sup>
$\text{V}_2\text{O}_5$ <sup>174</sup>	2	589	2–4.2 <sup>b</sup>
$\text{Mg}_{1.03}\text{Mn}_{0.97}\text{SiO}_4$ <sup>175</sup>	0.81	253	1.5–2.1 <sup>a</sup>
$\text{MgCoSiO}_4$ <sup>176</sup>	1	250 (at 700 °C)	1.2–2.0 <sup>a</sup>

<sup>a</sup> Potential measured vs.  $\text{Mg/Mg}^{2+}$ . <sup>b</sup> Potential measured vs.  $\text{Li/Li}^+$ .

rechargeable Mg batteries has focused on high-capacity Mg host cathodes and electrolytes. Possible cathode materials are summarized in Table 3.<sup>164,169,171–176</sup> Research has also been concentrated on electrolytes with wide electrochemical windows and reversible Mg dissolution-deposition.<sup>167,170,177,178</sup> However, a limited number of papers have been reported on anodes for rechargeable Mg batteries. Mg anode-related issues for rechargeable Mg batteries and Mg-ion batteries are discussed.

#### 3.1 Rechargeable Mg metal batteries

Incompatibility between Mg and the electrolyte has been thought of as the most difficult issue for rechargeable Mg batteries, since Mg naturally forms surface films upon exposure to oxygen, humidity, or most polar organic solvents. Unlike Li, the surface layer on Mg is a passivation barrier that insulates against both electrons and ionic species. Therefore, reversible Mg dissolution-deposition reactions do not occur in most polar organic electrolytes, such as those common in Li batteries. Mg can be electrochemically deposited and dissolved reversibly in solutions of Grignard reagents ( $\text{RMgX}$ , where R is an alkyl or aryl group, and X is Cl or Br) in ether,<sup>179,180</sup> since Mg electrodes are not passivated in such systems. However, the Grignard reagents cannot be used in battery systems due to their intrinsically strong reducing nature. Since reversible Mg dissolution-deposition reactions in  $\text{Mg}(\text{AlCl}_2\text{BuEt})_2/\text{THF}$  electrolytes were reported in 2000, much enthusiasm has been devoted to finding compatible electrolytes with reversible Mg dissolution-deposition reactions.

In contrast to Li metal anodes, Mg dendrite formation has not been observed during electrodeposition.<sup>181,182</sup> Aurbach *et al.* studied Mg deposition and dissolution processes using various analytical techniques, and demonstrated that the morphology of Mg deposition was strongly dependent on the composition of the electrolyte.<sup>181</sup> Also, an electrodeposition process of Mg metal from a Grignard-reagent-based electrolyte was compared with Li electrodeposition at various current densities.<sup>182</sup> The obtained Mg deposits did not show any dendritic morphology, as shown in Fig. 12, while all the Li deposits showed dendritic deposits under the same electrochemical conditions. An electrochemical study of the deposition-dissolution process of the Mg showed that the overpotential of Mg deposition had a significant dependency on the electrolyte concentration.

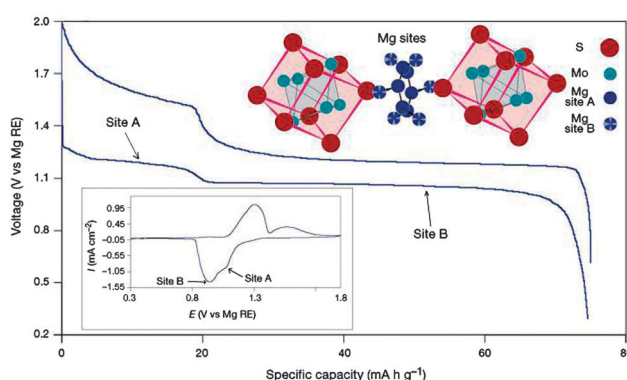


**Fig. 11** Typical electrochemical behavior and the basic structure of the  $\text{Mg}_x\text{Mo}_3\text{S}_4$  cathodes ( $0 < x < 1$ ) with the electrolyte of  $0.25\text{ M Mg(AlCl}_2\text{BuEt})_2$  in THF (inset: cyclic voltammogram of Mg insertion–extraction at  $0.05\text{ mV s}^{-1}$ ) (Nature Publishing Group, reprinted with permission).<sup>164</sup>

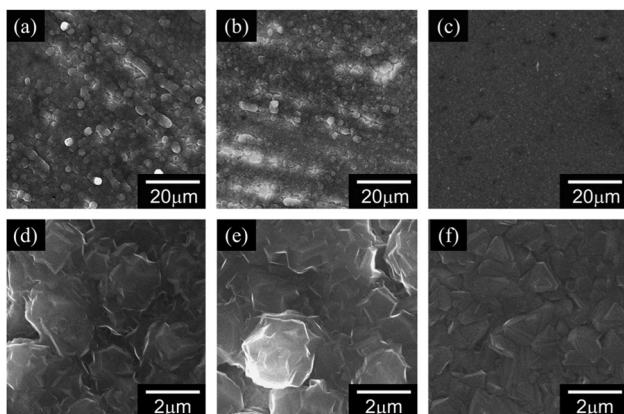


**Fig. 12** SEM images of the electrodeposited magnesium: (a) 500 $\times$ , 0.5 mA cm $^{-2}$ , (b) 500 $\times$ , 1.0 mA cm $^{-2}$ , (c) 500 $\times$ , 2.0 mA cm $^{-2}$ , (d) 5000 $\times$ , 0.5 mA cm $^{-2}$ , (e) 5000 $\times$ , 1.0 mA cm $^{-2}$  and (f) 5000 $\times$ , 2.0 mA cm $^{-2}$  (Science Direct, reprinted with permission).<sup>182</sup>

Various types of Mg alloys have been investigated as better alternatives to pure Mg metal in rechargeable Mg batteries.<sup>183</sup> The performances of Mg-alloys were dependent on the surface treatment prior to assembly. AZ61 alloy (6 wt% Al, 1 wt% Zn) showed good electrochemical performance with the highest Coulombic efficiency and the lowest resistance in coin cells among various Mg alloys. Although the highest resistance was observed with AP65 among these systems (6 wt% Al, 5 wt% Pb), it showed good Coulombic efficiency and reversible dissolution-deposition reaction.

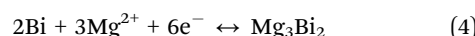
Nanostructured materials for rechargeable batteries provide enhanced kinetics because of their large surface areas, short diffusion lengths, and fast diffusion rates. The search for nanostructured Mg is a highly interesting topic for next-generation rechargeable Mg batteries.<sup>171,184</sup> Mg nanoparticles prepared using the ionic liquid-assisted chemical reduction method have been tested for reversibility with a graphite-like MoS<sub>2</sub> cathode in Mg(AlCl<sub>2</sub>Bu)<sub>2</sub>/THF electrolytes.<sup>184</sup> They exhibited high reversibility with a discharge capacity of 170 mA h g $^{-1}$  due to a decrease in the thickness of the passivating surface films, thus increasing Mg ion diffusion in the anode.

Owing to the metallic properties of Mg, physical modification methods such as ball milling, physical sputtering, and vapor deposition methods are more suitable for the preparation of nanostructured Mg than chemical modification methods. Recently, various physically modified nanostructured forms of Mg have been reported, such as Mg nanoblades<sup>185</sup> and 3D prism-like single-crystalline Mg nanostructures.<sup>186</sup> Although the nanostructured Mg has not yet been employed in the rechargeable Mg battery field, it could be applicable to secondary batteries for better electrochemical performance.

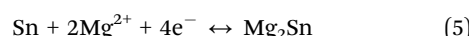
### 3.2 Rechargeable Mg-ion batteries

To compensate for the problems of Mg metal anodes, Mg-ion batteries have been suggested as an alternative solution. Matsui *et al.* reported electrodeposited bismuth (Bi), antimony (Sb), and Bi<sub>1-x</sub>Sb<sub>x</sub> alloys as anodes for Mg-ion batteries.<sup>187</sup> The Bi<sub>0.88</sub>Sb<sub>0.12</sub>

and Bi anodes showed good cycling performance over 100 cycles, while Sb showed poor reversibility, regardless of the morphology of the deposit, which suggested the importance of the Mg–M bond strength. Additionally, the reversible Mg<sup>2+</sup> insertion-extraction of the Bi electrode in an Mg(N(SO<sub>2</sub>CF<sub>3</sub>)<sub>2</sub>)/acetonitrile electrolyte demonstrated the compatibility of the Bi anode with conventional Mg-ion battery electrolytes. The following Mg reaction was possible with the Bi electrode:



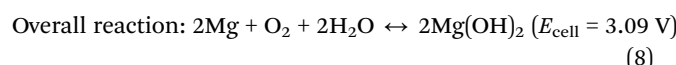
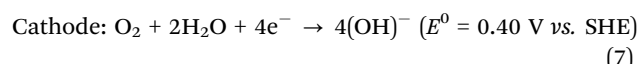
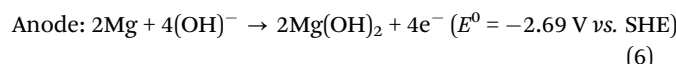
Recently, Sn was also suggested as a high-energy-density insertion-type anode material for rechargeable Mg-ion batteries.<sup>188</sup> The Sn anode showed higher capacities (903 mA h g $^{-1}$ ) and lower Mg<sup>2+</sup> insertion-extraction voltages (0.15/0.20 V vs. Mg/Mg<sup>2+</sup>). The electrochemical reaction between Mg and Sn can be expressed as follows:



Considering the many other binary Mg-based compounds, searches for higher-energy-density Mg-alloy-based anodes will be an important issue for solving the issues with rechargeable Mg-ion batteries.

### 3.3 Mg-air batteries

Mg-air batteries show promising properties, such as a high theoretical voltage of 3.09 V (in practice, the open circuit voltage is about 1.6 V) and an energy density of 2,840 W h kg $^{-1}$ . Although the Mg-air batteries have interesting advantages, only a few studies have focused on the development of the batteries. The reaction chemistry of Mg-air batteries in aqueous electrolytes is as follows:



The Mg-air batteries can be mechanically recharged, because the Mg electrode can be easily replaced.<sup>189,190</sup> The major problems in Mg-air battery systems are a low Coulombic efficiency of the Mg plate electrode, and high polarization during discharge. Therefore, to improve the battery performance in this system, the Mg electrode has to be modified to improve the electrochemical properties. Mg-Li and Mg-Li-Al-Ce alloys were suggested as potential materials for Mg-air battery anodes.<sup>190,191</sup> They showed higher electrochemical activity and a lower self-corrosion rate, which contributed to the higher operating voltage, anodic efficiency, and larger capacity than those with Mg and AZ31. Recently, Chen *et al.* reported on shape-controlled metallic Mg nano/meso-scale structured materials, such as Mg spheres, Mg plates, Mg nanorods, and sea-urchin-like Mg, which were prepared and applied to Mg-air battery systems, as shown in Fig. 13.<sup>192</sup>

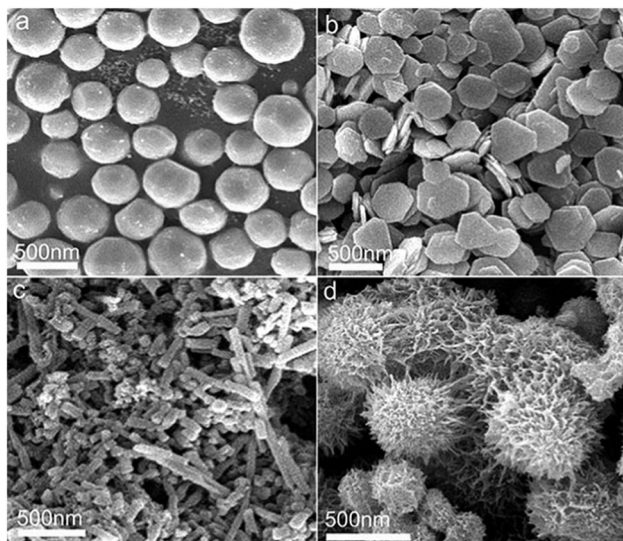


**Fig. 13** Typical scanning electron microscopy (SEM) images of the various nanostructured Mg: (a) Mg spheres, (b) Mg plates, (c) Mg nanorods, (d) sea urchin-like Mg (The John Wiley & Sons, Inc., reprinted with permission).<sup>192</sup>

The results showed that Mg sea-urchin-like nanostructure with the highest specific surface area displayed much better electrochemical performance and high energy density.

### 3.4 Mg–Sb liquid metal batteries

An all-liquid Mg–Sb metal battery operating at a high temperature of 700 °C comprising an Mg negative electrode, a molten salt electrolyte ( $MgCl_2$ – $KCl$ – $NaCl$ ), and an Sb positive electrode was proposed and characterized.<sup>193</sup> Because of differences in density and immiscibility, the salt and metal phases were divided into three distinct layers (Fig. 14), and the following reaction chemistry was suggested:

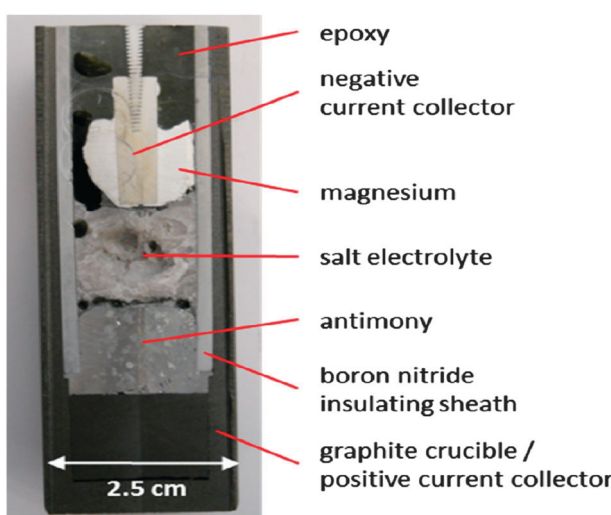
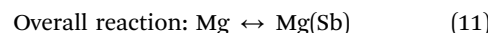
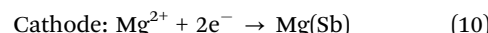
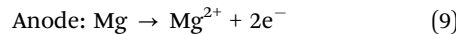


**Fig. 14**  $Mg||Sb$  liquid metal battery operated at 700 °C showing the three stratified liquid phases upon cooling to room temperature. The cell was filled with epoxy prior to sectioning (The American Chemical Society, reprinted with permission).<sup>193</sup>



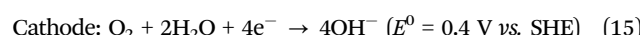
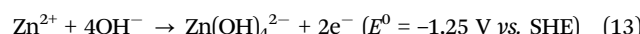
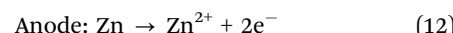
At the negative electrode, Mg is oxidized to  $Mg^{2+}$  during discharge, while at the positive electrode,  $Mg^{2+}$  ions in the electrolyte are reduced to Mg, which is deposited onto the Sb electrode to form a liquid metal alloy of  $Mg(Sb)$ . During the charge step, the reverse reactions occur. Prepared cells were cycled under constant current conditions, and demonstrated high rate capabilities and negligible corrosion of the solid-state cell components over the testing period.

## 4. Metallic zinc (Zn) electrode

The Zn electrode is one of the most widely used metallic electrodes. Zn has various advantageous features of abundance, low cost, environmental benignity, ease of handling, relatively low equilibrium potential, stability in aqueous electrolytes, and good electrochemical equivalence of 820 Ah kg<sup>-1</sup>.<sup>165</sup> Therefore, Zn has been a material of choice for battery anodes for more than two centuries. There are several commercial Zn-based battery systems, such as Zn– $MnO_2$ , Zn–AgO, Zn–HgO, Zn–air, and Ni–Zn. Each of the systems has its own unique advantages in certain market sectors.<sup>165,194</sup> Among these battery systems, Zn–air and Ni–Zn can be used as rechargeable batteries, and research has been conducted to enhance their electrochemical performance. This section focuses on issues related to Zn anodes for rechargeable Zn-based batteries.

### 4.1 Rechargeable Zn–air( $O_2$ ) batteries

Zn–air batteries show the highest specific energy density compared with other Zn-based alkaline batteries, which is due to the unlimited supply of oxygen from air. The theoretical specific energy density of Zn–air batteries is 1086 W h kg<sup>-1</sup>. The overall cell discharge reactions for a Zn–air( $O_2$ ) rechargeable battery using a Zn anode and an air cathode in KOH electrolyte solution can be summarized as follows:<sup>165,194–196</sup>

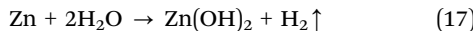


Secondary Zn–air( $O_2$ ) batteries can be classified into mechanically and electrically rechargeable batteries.<sup>165,197</sup> The mechanically rechargeable batteries are designed with a means to remove and replace the discharged anodes or discharge products, and can be recharged externally. This avoids the need for a bi-functional air cathode for charge–discharge, and addresses problems with the shape change of the Zn anode resulting from repeated cycling. In contrast, electrically rechargeable batteries use an air cathode with a bi-functional

catalyst, and the charge-discharge process takes place within the battery structure. A satisfactory system with electrical recharging would feature low material cost and high specific energy. However, making electrically rechargeable Zn-air batteries is still challenging.<sup>165,194,198</sup> Although a proper bi-functional catalyst is required to charge a Zn-air battery with lower electrical potential, it is also critical for obtaining reversible zinc anodes.

Zn metal undergoes shape change during repeated charge-discharge, which includes the formation of dendrites, non-uniform zinc dissolution, and limited solubility in electrolytes.<sup>199–206</sup> To prevent dendrite formation, intensive research has been reported, and has mainly involved three types of methods: separator modification, additives in the electrode/electrolyte, and AC or pulsed charging.<sup>207</sup> Among these, additives in the electrode/electrolyte have attracted the most attention, and can be divided into three categories: (i) structural electrode modifiers, (ii) metallic additives, and (iii) organic additives.<sup>207–212</sup> As structural electrode modifiers, 3-D structures using polytetrafluoroethylene or graphite were reported. These modifiers could help to trap the dissolved Zn species ( $\text{Zn(OH)}_4^{2-}$ ,  $\text{Zn}^{2+}$ ) in the vicinity of the electrode upon discharge.<sup>208–211</sup> The metallic additives include metal or metallic oxide/hydroxide, such as Pb, Sn, Hg,  $\text{HgO}$ ,  $\text{CdO}$ ,  $\text{PbO}$ ,  $\text{Bi}_2\text{O}_3$ ,  $\text{Ga}_2\text{O}_3$ ,  $\text{Tl}_2\text{O}_3$ ,  $\text{Ca(OH)}_2$ , and  $\text{In(OH)}_3$ , which can be reduced to the metal prior to the reduction of zincate ( $\text{Zn(OH)}_4^{2-}$ ).<sup>212–215</sup> These metallic additives increased the polarizability of the electrode, which improved the current distribution and decreased the shape change. The organic additives can be adsorbed on the electrode surface, specifically at the sites of rapid growth (*i.e.*, dendrites).<sup>216–221</sup> The adsorbed organic species precluded or slowed down further growth of dendrites. The effects of tetrabutylammonium bromides,<sup>217</sup> tetra-alkyl ammonium hydroxides,<sup>218</sup> triethanolamine,<sup>219</sup> and Triton X-100<sup>220</sup> were proposed and tested as inhibitors of Zn-dendrite growth. The use of anions of organic acids, such as phosphoric acid, tartaric acid, succinic acid, and citric acid, was also suggested for suppressing dendrite formation.<sup>221</sup>

Since Zn has a more negative reduction potential than hydrogen, it spontaneously generates  $\text{H}_2$  gas evolution reaction (HER) on the surface of Zn particles in an aqueous medium. The HER in an alkaline battery is given below.<sup>195,222–225</sup>



The HER on the Zn metal surface deteriorates the efficiency of the Zn, and decreases the cycle life of the Zn-air battery. To solve this problem, several methods were suggested, involving the coating of various additives on the surface of Zn metal, and the alloying of Zn metal with other metals that have a high hydrogen evolution overpotential.<sup>226</sup> Although several metals have been demonstrated to alleviate the HER, such as Hg, Pb, and Cd, their uses are prohibited due to environmental issues.<sup>226,227</sup> Additives using metal or metal compounds have also been proposed. Environmentally friendly Bi, Ni, and In were effective for increasing the overpotential of HER at the Zn anode, which could replace Hg and Pb in Zn alloy powders.<sup>228–230</sup> Metallic Bi incorporated into a pasted Zn electrode also improved

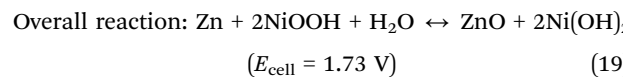
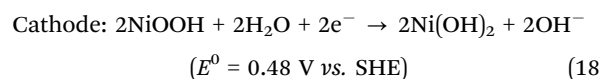
the discharge performance by the formation of an electronic conductive material.<sup>229</sup> Recently, several Zn–Ni–In alloys were used for the reduction of dendrite formation and hydrogen evolution.<sup>230</sup> Gelling agents such as cross-linked carboxymethyl cellulose, starch graft copolymers, cross-linked polyacrylic acid polymer, and organic binders were also suggested to optimize and stabilize Zn electrodes.<sup>231–234</sup>

During the discharge reaction of a Zn-air battery,  $\text{Zn(OH)}_4^{2-}$  is transformed into  $\text{ZnO}$ , which acts as an insulator. To develop a rechargeable Zn-air battery, the electrochemical behavior of the  $\text{Zn(OH)}_4^{2-}$  in alkaline solution has to be clarified.<sup>165</sup> To understand the behavior and electrodeposition of the  $\text{Zn(OH)}_4^{2-}$  in an alkaline electrolyte, several fundamental studies have been reported.<sup>200,203,204,222,235–237</sup> The mechanism of zinc electroplating and the sequential transformation of  $\text{Zn(OH)}_2$  to  $\text{Zn(OH)}_{\text{ad}}$  and Zn was studied by Peng,<sup>237</sup> and Einerhand *et al.*,<sup>222</sup> who demonstrated increased hydrogen evolution with the decreasing concentration of KOH and  $\text{Zn(OH)}_4^{2-}$ .

The most practical method for improving the electrochemical performance of the Zn anode is to increase the surface area through the modification of zinc particles, which provides more efficient electrochemical reaction of Zn in the alkaline electrolyte. Several approaches for controlling the morphology of zinc metal, such as Zn-fibers and Zn-dendrites, have been reported, showing enhanced electrochemical performance.<sup>238,239</sup> Additionally, porous electrodes with zinc particles of various shape, not just planar zinc electrodes, also showed improved charge-discharge behaviors.<sup>240</sup> The preparation of various nanostructured Zn has been reported and applied to several Zn-based battery systems, which showed enhanced cycling behaviors.<sup>226,241</sup> Although the nanostructured Zn has not been applied to Zn-air battery systems, it will be helpful for obtaining better performance if applied to Zn-air batteries.

#### 4.2 Rechargeable Ni–Zn batteries

The Ni–Zn battery is an alkaline rechargeable battery system, which has drawn much attention for its high energy density, high power density, high working voltage, wide working temperature range, abundant raw material, and lack of environmental pollution in production and application. Since 2000, the development of a stabilized Zn electrode system has made this technology viable and competitive with other commercial rechargeable battery systems, such as Pb-acid, Ni–Cd, and Ni–MH.<sup>151</sup> Although rechargeable Ni–Zn batteries were commercialized by Powergenix,<sup>242</sup> intensive research efforts have been conducted to enhance their electrochemical properties. The anodic reactions involved in the alkaline electrolyte would be the same as those in a Zn-air battery (reactions (12)–(14)). The cathodic and overall cell reactions for the Ni–Zn battery using a Zn anode and a Ni cathode in KOH electrolyte solution can be summarized as follows:<sup>165,243,244</sup>



ZnO powders show a tendency to dissolve in KOH solution to form a soluble zincate.<sup>244</sup> During the discharge process of a Zn electrode, Zn releases electrons to form the zincate by charge transfer reaction. At the same time, the concentration of the zincate in the KOH solution increases, which leads to precipitation of the zincate to form ZnO. In contrast, the reaction of a rechargeable Ni/MH battery involves hydrogen diffusion in the interior of the alloy powder and charge transfer reaction at the alloy powder surface during discharge. The hydrogen atoms are adsorbed at the surface of the alloy powder in the charging process to form adsorbed hydrogen atoms ( $H_{ads}$ ), which diffuse into the interior of the alloy to become adsorbed hydrogen atoms ( $H_{abs}$ ).

A Zn electrode can be prepared in either charged or discharged states depending on whether the starting material is metallic Zn (charged) or ZnO (discharged). Typically, charged Zn electrodes are used only in primary batteries, while secondary batteries are usually manufactured in the discharged state.<sup>165</sup> Therefore, the investigation of the reaction mechanism for the formation of ZnO in rechargeable Ni-Zn batteries is a very important issue to improve its electrochemical performance. The most critical problems of Ni-Zn rechargeable batteries are their relatively low cycle life, self-discharge, and discharge capacity fading, which are attributed to the shape change of the Zn electrode and Zn corrosion.<sup>199–206,245–247</sup> These disadvantages are similar to those of a Zn anode in a Zn-air battery system. Research has been carried out to overcome the shape change and dissolution problems of the Zn electrode.

One approach is to add additives to either the electrode or the electrolyte.<sup>212,213,248–251</sup> A physical mixture of ZnO and metal or metal oxides, such as Ag,<sup>248</sup> Ni,<sup>249</sup> SnO<sub>2</sub>,<sup>213</sup> Bi<sub>2</sub>O<sub>3</sub>,<sup>211</sup> CdO,<sup>250</sup> and PbO,<sup>251</sup> was suggested to improve the electrochemical performance of Zn electrodes. Enhanced charge-discharge behaviors were demonstrated, because the additives reduced the zincate concentration, provided an improved substrate for Zn electrodeposition, enhanced the electronic conductivity, and enabled a uniform current distribution. Also, the addition of calcium hydroxide, Ca(OH)<sub>2</sub>, to the Zn electrode led to a decrease of the zincate concentration and an increase of the cell life.<sup>252,253</sup> The reason was that Ca(OH)<sub>2</sub> reacted with the discharge product of ZnO to yield calcium zincate, Ca(OH)<sub>2</sub>·2Zn(OH)<sub>2</sub>·2H<sub>2</sub>O.

However, these physical mixtures could not provide a homogeneous mixture and tight contact between the additives and ZnO particles, so the efficiency of the additives was relatively low. In addition, some additives with poor electronic conductivity would increase the internal resistance of the battery, and result in insufficient drainage of charges within the active material during recharging. Recently, several studies for homogeneous and tight contact between additives and ZnO have been reported. Ca(OH)<sub>2</sub>-coated ZnO and ZnO/conductive-ceramic nanocomposites were prepared by direct precipitation methods,<sup>254,255</sup> which showed better cycling stability and higher discharge capacities compared with pure ZnO and physical mixtures of ZnO/additives. TiO<sub>2</sub>-coated ZnO prepared by the sol-gel method at various temperatures showed improved physicochemical and electrochemical properties,

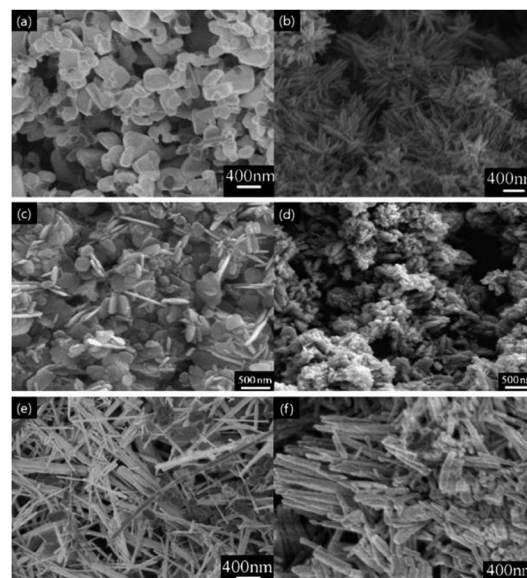


**Fig. 15** Morphology evolution process of various nanostructured ZnO: (a) conventional ZnO before cycling and (b) after 40 cycles, (c) ZnO nanoplates before cycling and (d) after 67 cycles, and (e) ZnO nanowires before cycling and (f) after 75 cycles (Science Direct, reprinted with permission).<sup>259,260</sup>

since the passive surface layer effectively reduced the dissolution of Zn, which caused self-discharge and capacity fading. The modified ZnO suppressed the shape change and the formation of dendrites.<sup>256</sup> K<sub>2</sub>CO<sub>3</sub> and KF were also suggested as additives in the alkaline electrolytes, which could partially solve the problems of shape change and dendritic shorting of the Zn electrode by reducing the solubility of Zn in the electrolyte.<sup>257</sup>

Research on nanostructured ZnO has shown the enhancement of the charge-discharge behaviors of Zn electrodes. Acicular crystalline ZnO showed improved cycling behavior, since Zn grains were kept from becoming extremely large, and suppressed the dendrite formation of the Zn electrodes.<sup>258</sup> ZnO nanowires and nanoplates were prepared by hydrothermal routes, and improved cycle performance was observed in comparison with conventional ZnO. Conventional ZnO showed distinct dendrite formation after cycling, whereas the ZnO nanoplates and ZnO nanowires did not change their morphology, and Zn dendrites were suppressed effectively after repeated cycling (Fig. 15).<sup>259,260</sup> The ZnO nanowires intertwined readily and decreased the contact resistance among electrode materials. The nanoplate ZnO had excellent plasticity, creep resistance, and the fastest growth in the  $\langle 11\bar{2}0 \rangle$  direction, in addition to impeding dendritic formation.

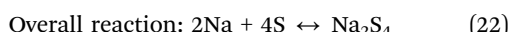
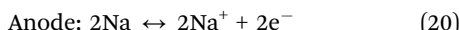
## 5. Other battery systems based on metallic anode materials

There have been continuous efforts to make the electric grid more stable and reliable in energy storage systems (ESSs) using rechargeable batteries. ESSs are used to store excess electricity during off-peak hours, which is released during peak hours.

ESSs are significantly beneficial for reducing the need for peak generation, as well as strain on transmission and distribution networks. ESSs can also provide critical auxiliary functions to render renewable energy more efficient by frequency regulation and voltage support.

### 5.1 Na–S battery

Among various ESSs, sodium–sulfur (Na–S) batteries have been intensively explored due to their high energy density, high cycling efficiency, and long-term reliability. An Na–S battery can be fabricated using abundant and inexpensive materials. The first Na–S battery was developed in the 1960s by the Ford motor company.<sup>261–263</sup> The Na–S battery consists of an Na anode, an S cathode, and a beta alumina solid electrolyte (BASE), which operates around 300 °C. At such a high temperature, both Na and S exist in a molten state, and S is absorbed in a carbon sponge or graphite felt. During the discharge, molten metallic Na loses an electron, and the  $\text{Na}^+$  ion migrates to the S container through the BASE. During the charge, the reverse process takes place, and these processes can be expressed as follows with a 2 V cell voltage:



In a typical structure of a Na–S battery, the molten Na and S are placed in concentric cylindrical containers separated by metals and the BASE, with Na in the center and S on the outside, as shown in Fig. 16. Because of the high reactivity of Na and S, each cell is sealed to prevent leakage.

From a material perspective, modification of this type of battery has mainly focused on the solid electrolyte. There are two types of crystal structures in BASE, which are  $\beta\text{-Al}_2\text{O}_3$  (hexagonal;  $P6_3/mmc$   $a = 0.559$  nm,  $c = 2.261$  nm) and  $\beta''\text{-Al}_2\text{O}_3$  (rhombohedral;  $R3m$   $a = 0.560$  nm,  $c = 3.395$  nm).<sup>264,265</sup> The unit cell of  $\beta''\text{-Al}_2\text{O}_3$  is 50% larger than that of  $\beta\text{-Al}_2\text{O}_3$ , and shows higher  $\text{Na}^+$  conductivity. The stoichiometry of BASE can be expressed as  $(\text{Na}_2\text{O})\cdot 11\text{Al}_2\text{O}_3$ . Due to its thermodynamically

metastable nature, dopants such as  $\text{MgO}$  or  $\text{Li}_2\text{O}$  are generally used to stabilize the crystal structure.<sup>266,267</sup> A highly dense form of BASE is required to achieve high ionic conductivity and mechanical strength, and these properties are closely related to its microstructural characteristics such as the particle size and porosity. The synthesis of conventional BASE is carried out by the solid-state reaction of  $\alpha\text{-Al}_2\text{O}_3$  with  $\text{Na}_2\text{CO}_3$  and  $\text{MgO}$ , and/or  $\text{Li}_2\text{O}$  as a stabilizer.<sup>268</sup> The solid-state reaction, however, had a disadvantage in that a two-phase mixture of  $\beta$  and  $\beta''\text{-Al}_2\text{O}_3$  was formed, and complex post treatments were often necessary to obtain a single-phase material.

Instead of this conventional method, syntheses of  $\beta''\text{-Al}_2\text{O}_3$  through soft-chemistry such as sol–gel method,<sup>269</sup> co-precipitation,<sup>270</sup> and spray-freeze/freeze-drying<sup>271</sup> have also been reported. In these methods, single-phase  $\beta''\text{-Al}_2\text{O}_3$  can be obtained only after post heat treatment for several hours at high temperature, since sintering below 1850 K does not provide the required properties. High-temperature sintering would lead to the loss of Na, resulting in compositional variation with lower conductivity, which is not suitable for solid electrolytes. The solution combustion method<sup>272</sup> can yield a single-phase  $\beta''\text{-Al}_2\text{O}_3$  at much lower temperatures such as 773 K, but a subsequent higher-temperature heat treatment is needed. In order to overcome this problem, microwave synthesis has been employed for simultaneous synthesis and sintering. Subasri *et al.* demonstrated that a single phase of  $\beta\text{-Al}_2\text{O}_3$  or  $\beta''\text{-Al}_2\text{O}_3$  could be prepared using microwaves to produce a high-density phase within a short period of time.<sup>273</sup>

The mechanical strength of BASE is also affected significantly by abnormally grown grains, as well as defects such as voids, cracks, and impurities, which can result in crack generation and propagation sites. The fracture toughness of BASE can also be improved by the incorporation of  $\text{ZrO}_2$ , which leads to an increase of the critical current density, and thus improved battery performance characteristics such as cycle life and rate capability.<sup>274</sup> Because  $\text{ZrO}_2$  is not an  $\text{Na}^+$  conductor at the battery operating temperature, excessive  $\text{ZrO}_2$  is harmful to the battery performance.

The  $\text{Na}^+$  ion conductivity of  $\beta''\text{-Al}_2\text{O}_3$  is also influenced by the microstructure and impurities.<sup>275</sup> As the average particle size decreases, the fracture toughness increases, and the  $\text{Na}^+$  ion conductivity decreases. Impurities such as Ca and Si form undesirable phases of calcium aluminate and aluminum silicate on the grain boundaries, respectively, resulting in an increase of resistance. Ca also induces incomplete wetting between the liquid Na anode and the electrolyte. Despite considerable technical improvements, the BASE system cannot be adapted for low-temperature applications. To compensate for the drawbacks of BASE, a low-temperature  $\text{Na}^+$  ion conductor was recently reported. Ceramatec reported the achievement of an Na–S battery system operating at 120 °C, which employed a NASICON-type electrolyte with conductivity on the order of  $10^{-2}$  S cm<sup>-1</sup>.<sup>276</sup> Hayashi *et al.* studied an  $\text{Na}_3\text{PS}_4$  superionic conductor, which showed  $\text{Na}^+$  ion conductivity of over  $10^{-4}$  S cm<sup>-1</sup> at room temperature. They constructed an all-solid-state cell ( $\text{Na}-\text{Sn}/\text{Na}_3\text{PS}_4/\text{TiS}_2$ ), which operated as a rechargeable sodium battery at room temperature with an average cell voltage of 1.6 V.<sup>277</sup>

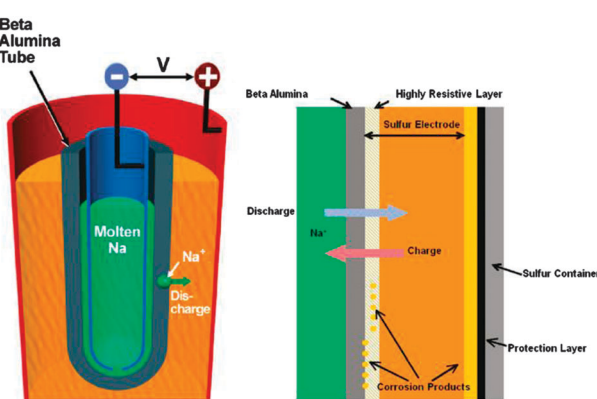
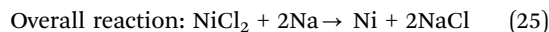
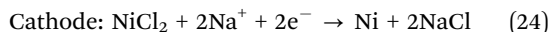
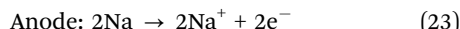


**Fig. 16** Schematics of the structure and electrochemical reactions of a Na–S battery system (The American Chemical Society, reprinted with permission).<sup>261</sup>

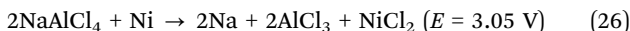
Although Na-S batteries have been investigated for a long time, they still have some shortcomings. The primary disadvantage is safety. If the BASE electrolyte is broken, an internal short between the anode and the cathode occurs, and the cell may explode. Also, sodium polysulfide is highly corrosive and attacks the container, which requires an effective protective coating. Because of this corrosive environment, it is not possible to fabricate planar cells, and the design is restricted to tubular cells. High-cost conducting components are also needed for the cathode to provide sufficient electronic conductivity due to the insulating nature of the S electrode.

### 5.2 Na-NiCl<sub>2</sub> battery

To overcome these disadvantages of the Na-S battery, another liquid Na-based battery system was invented using Na-NiCl<sub>2</sub> in 1978, and was called the ZEBRA battery (Zeolite applied to Battery Research Africa).<sup>278</sup> Since the Na-NiCl<sub>2</sub> battery employed the same anode and electrolyte as those of the Na-S battery, it operated under almost the same conditions. The reactions at each electrode and the overall cell reactions were as follows with a cell voltage of 2.58 V at 300 °C:



Because the BASE and metal halide in the cathode were in solid states, molten NaAlCl<sub>4</sub> was used as an auxiliary electrolyte to enhance the contact between BASE and the cathode, thus promoting Na<sup>+</sup> ion transport. Unlike sodium polysulfide, metal halide is not so corrosive, resulting in fewer restrictions on the choice of cell component materials for this system. The Na-NiCl<sub>2</sub> battery is relatively safe compared to the Na-S battery. Once BASE is broken, NaAlCl<sub>4</sub> reacts with Na to form Al and NaCl, which could seal small cracks. If a crack is large enough and cannot be sealed by NaCl, there would be a soft short-circuit by Al, and the cell voltage drops without cell breaking. Even in this case, the cell still operates. Another advantage of this battery regarding safety is that it protects BASE under overcharge conditions by reacting Ni with NaAlCl<sub>4</sub> to form Na and metal halides,



By adding a small amount of NaBr and NaI, Na<sup>+</sup> ion transport was enhanced, and cell performance was improved. Al, Fe, and FeS were also helpful for increasing cell performance by stabilizing the cathode.<sup>279</sup> Another metal halide cathode such as FeCl<sub>2</sub> was also explored, but BASE degradation and overcharge sensitivity had to be solved for adaptation as an alternative to NiCl<sub>2</sub> cathodes.<sup>280</sup>

### 5.3 Na-air(O<sub>2</sub>) battery

Recently, Na-air(O<sub>2</sub>) battery systems have also gained attention as a high-energy-density Na secondary battery for electric vehicle applications.<sup>7,281–283</sup> The theoretical cell voltage is 2.33 V (with Na<sub>2</sub>O<sub>2</sub> as a final product), with a theoretical energy

density of 1605 W h kg<sup>-1</sup>, which is much higher than that of currently used Li-ion batteries.<sup>7</sup> Peled *et al.* demonstrated an Na-O<sub>2</sub> battery that operates above the melting point of the Na metal anode,<sup>281</sup> which showed a working cell voltage of 1.75 V, and required 3.0 V during charging. They stated that the use of a liquid Na anode at elevated temperature had some advantages compared to an Li metal anode, by acceleration of the sluggish cathode reactions, lowering of the cell impedance, elimination of dendrite formation, minimization of the interference by water vapor and CO<sub>2</sub>, and utilization of light and low-cost hardware materials like aluminum. In order to prove that molten Na could be cycled, the electrochemical performance of a liquid Na metal anode was investigated at 105 °C using a coin cell composed of Na triflate (NaCF<sub>3</sub>SO<sub>3</sub>)/polyethylene oxide (PEO) polymer electrolyte/Al. While the liquid Na anode was cycled for over 140 cycles, the Coulombic efficiency of the liquid Na anode during cycling was about 85% for each cycle, which is too low for the commercialization of the battery system. Moreover, there are some technical issues with the use of liquid Na anodes, since liquid Na is highly corrosive, and operation at high temperature is impractical.

In order to address problems related to liquid Na anodes, Sun *et al.* demonstrated a room-temperature Na-air battery system using an Na metal anode and a diamond-like carbon (DLC) thin film as an air electrode.<sup>282</sup> The gravimetric capacities of the Na-air battery operated at room temperature were 1884 mA h g<sup>-1</sup> (565 μA h cm<sup>-2</sup>) at 1/10 C and 3600 mA h g<sup>-1</sup> (1080 μA h cm<sup>-2</sup>) at 1/60 C. Only 56% of the initial capacity was retained after 20 cycles, and this system still suffered from poor cycle performance. Hartmann *et al.* reported a significant improvement of Na-air batteries by replacing the organic carbonate solvent with diethylene glycol dimethyl ether.<sup>7</sup> The Na-air battery system showed reversible charge and discharge with a relatively low overpotential of about 200 mV and current densities as high as 0.2 mA cm<sup>-2</sup>, even without any catalyst for the air cathode. Better electrochemical kinetics of the Na-air battery system could be obtained compared to that of the Li-air battery system (Fig. 17). It was also shown that crystalline Na superoxide (NaO<sub>2</sub>) formed in a single-electron transfer step as a solid discharge product, indicating that the reaction mechanism of the Na-air battery differs from that of the Li-air battery system. Even though the capacity retention of the Na-air battery is still poor, these results showed that the Na-air battery system deserves to be regarded as a promising candidate for next-generation battery systems. However, the use of Na metal anodes should be carefully investigated in terms of safety and reliability, because of the low melting point of Na metal (~98 °C) and its high reactivity. This battery safety issue could be solved by using an alternative battery material that can guarantee safe operation of Na-based secondary batteries, including a Na<sup>+</sup> conducting solid-state electrolyte and Na-alloy systems such as Na-Sn alloy.<sup>284</sup>

### 5.4 Al-air(O<sub>2</sub>) battery

Al-air(O<sub>2</sub>) battery systems have been regarded as a promising system for electric vehicles, because of their high theoretical

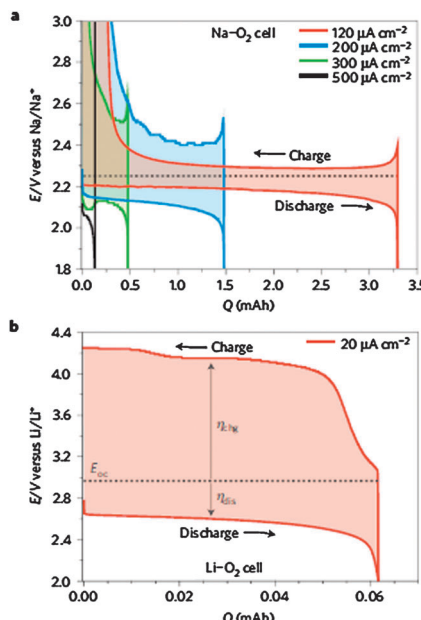


**Fig. 17** Electrochemical characterization of  $\text{Na}-\text{O}_2$  (a) and  $\text{Li}-\text{O}_2$  (b) cells with a gas diffusion layer cathode (Nature Publishing Group, reprinted with permission).<sup>7</sup>

energy density ( $2793 \text{ W h kg}^{-1}$ ) with a theoretical cell voltage of  $2.71 \text{ V}$ .<sup>285</sup> In addition, Al anodes have advantages such as low cost, environmentally friendliness, and recyclability. However, there are some problems to be solved for practical use of Al-air battery systems. First of all, the working voltage of Al-air batteries is too low (about  $1.3 \text{ V}$ ) compared to the theoretical value,<sup>286</sup> because Al anodes cannot be operated at the equilibrium potential of Al due to unwanted side reactions between Al and  $\text{H}_2\text{O}$ . Al-air battery systems using aqueous electrolytes also cannot be recharged, and only mechanical charging (replacing the discharged Al anode with a new Al anode) is possible.

Despite these challenges, Al-air battery systems deserve to be considered as a potential candidate for EV power sources. Yang *et al.* reported that a cost as low as  $\$1.1 \text{ kg}^{-1}$  could be achieved with Al anodes if the discharge product can be recycled, and the energy efficiency of the Al-air system could be comparable to that of an internal combustion engine through a design analysis of the Al-air battery for EVs, in terms of cost, life-cycle, and energy density.<sup>286</sup> They also showed that Al-air battery systems could have a driving range comparable to that of internal combustion engines. Considering that the production cost of a battery and driving range are key success factors for the commercialization of electric vehicles, Al-air battery systems still have potential as a power source for EVs. There are some inherent issues when Al anodes are used, including the reversibility of Al anodes during cycling (reversible electrodeposition and dissolution) and the inhibition of Al corrosion with the electrolyte. Recent progress in electrochemical technology with non-aqueous electrolytes such as room-temperature ionic liquids will be helpful to address the issues with Al anodes for Al-air battery systems.

## 6. Summary

Recent applications for EVs and large-scale energy storage systems have increased the demand for high-electrochemical-performance materials for anodes, cathodes, and electrolytes with other components in rechargeable batteries. Widespread usage of EVs employing current Li-ion batteries has been delayed due to their insufficient energy density and the high cost of large-scale Li-ion batteries. Secondary batteries employing metallic anode materials generally have higher volumetric and/or gravimetric energy densities, and are promising candidates to replace Li-ion batteries and to increase the driving range of EVs.

However, even though extensive research has been carried out to solve the problems associated with metallic anodes, especially for Li metal, commercialization is still hindered by the many technical issues left to be solved. The poor cycle performance of metallic anode material is one of the most important issues, as well as reliability and safety concerns. In this *review*, we have presented the closely related unresolved issues such as the underlying reaction mechanism of Li dendrites and the development of physicochemically stable passivation layers for Li electrodes for Li-metal-based secondary batteries. These issues are of the utmost importance for realizing widespread usage of EVs and large-format electricity storage for renewable energy, as well as for the commercialization of Li-air and Li-S batteries. Li metal electrodes with high reversibility and safety would be exploited as anodes for currently used Li-ion batteries, since the theoretical gravimetric energy density of current Li-ion batteries could be almost doubled if Li metal anodes could be successfully adopted. For example, the maximum gravimetric energy density of an  $\text{Li}-\text{MnO}_2$  cell is about  $712 \text{ W h kg}^{-1}$ , which is 184% larger than that of graphite-LiCoO<sub>2</sub> cells. This fact indicates that it is not necessary to modify the currently used Li-ion battery cell configuration, thereby suppressing the increase in the production cost associated with the further installation of assembly lines for newly designed cell configurations such as Li-air batteries. Also prelithiated metallic or Li-containing non-metallic materials should be exploited as anode materials for Li-S and Li-air batteries.

Mg and Zn metallic anodes have gained much attention as anode materials for Zn- and Mg-based secondary batteries, because of their abundance, low cost, and high theoretical energy density, especially for metal-air batteries. Although these electrodes have shown improved electrochemical performance along with the recent progress, there are still many technical issues to be overcome for commercialization. Zn electrodes have shape-change problems, as well as technical problems similar to those of Li electrodes, such as dendritic growth of Zn during cycling, and irreversible chemical reaction with the electrolyte. Even though Mg electrodes do not show severe shape changes during cycling, the use of Mg electrodes as an anode for Mg secondary batteries is still hindered by irreversible chemical reaction of the Mg electrode. Proper design of electrode and electrolyte materials in terms of microstructure, composition, reaction chemistries, and shape control based on comprehensive knowledge of the underlying reaction

mechanisms is required to further advance the employment of metallic anode materials for next-generation secondary batteries.

## Notes and references

- 1 LIB-related Study, Program 2010–2011, Institute of Information Technology, Ltd., Japan, 2011.
- 2 C.-M. Park, J.-H. Kim, H. Kim and H.-J. Sohn, *Chem. Soc. Rev.*, 2010, **39**, 3115.
- 3 N. Choi, Z. Chen, S. A. Freunberger, X. Ji, Y.-K. Sun, K. Amine, G. Yushin, L. Nazar, J. Cho and P. G. Bruce, *Angew. Chem., Int. Ed.*, 2012, **51**, 9994.
- 4 G. Jeong, Y.-U. Kim, H. Kim, Y.-J. Kim and H.-J. Sohn, *Energy Environ. Sci.*, 2011, **4**, 1986.
- 5 P. G. Bruce, S. A. Freunberger, L. J. Hardwick and J.-M. Tarascon, *Nat. Mater.*, 2012, **11**, 19.
- 6 R. Black, B. Adams and L. F. Nazar, *Adv. Energy Mater.*, 2012, **2**, 801.
- 7 P. Hartmann, C. L. Bender, M. Vracar, A. K. Durr, A. Garsuch, J. Janek and P. Adelhelm, *Nat. Mater.*, 2013, **12**, 228.
- 8 J.-I. Yamaki and S.-I. Tobishima, in *Handbook of Battery Materials*, ed. C. Daniel and J. O. Bessenhard, Wiley-VCH Verlag & Co. KGaA, Weinheim, Germany, 2011, ch. 13.
- 9 C. Wang, D. L. Wang and C. S. Dai, *J. Electrochem. Soc.*, 2008, **155**, A390.
- 10 F. Orsini, A. D. Pasquier, B. Beaudoin, J. M. Tarascon, M. Trentin, N. Langenhuizen, D. E. Beer and P. Notten, *J. Power Sources*, 1998, **76**, 19.
- 11 J. M. Tarascon and M. Armand, *Nature*, 2001, **414**, 359.
- 12 U. V. Sacken, E. Nodwell, A. Sundher and J. R. Dahn, *Solid State Ionics*, 1994, **69**, 284.
- 13 D. Aurbach, *Nonaqueous Electrochemistry*, Marcel Dekker, New York, 1999.
- 14 F. C. Laman and K. Brandt, *J. Power Sources*, 1988, **24**, 195.
- 15 K. Brandt, *Solid State Ionics*, 1994, **69**, 173.
- 16 L. F. Nazar and O. Crosnier, in *Lithium Batteries Science and Technology*, ed. G.-A. Nazri and G. Pistoia, Springer, New York, 2009, ch. 4.
- 17 A. N. Dey and E. J. Rudd, *J. Electrochem. Soc.*, 1974, **121**, 1294.
- 18 R. D. Rauh and S. B. Brummer, *Electrochim. Acta*, 1977, **22**, 75.
- 19 K. M. Abraham, *Electrochim. Acta*, 1993, **38**, 1233.
- 20 Z.-I. Takehara, *J. Power Sources*, 1997, **68**, 82.
- 21 E. Peled, *J. Electrochem. Soc.*, 1979, **126**, 2047.
- 22 K. Kanamura, S. Shiraishi and Z.-I. Takehara, *J. Electrochem. Soc.*, 1994, **141**, L108.
- 23 D. Aurbach, B. Markovsky, A. Schechter, Y. Ein-Eli and H. Cohen, *J. Electrochem. Soc.*, 1996, **143**, 3809.
- 24 D. Aurbach, I. Weissman, A. Schechter and H. Cohen, *Langmuir*, 1996, **12**, 3991.
- 25 D. Aurbach, O. Chusid and I. Weissman, *Electrochim. Acta*, 1996, **41**, 747.
- 26 M. Odzimekowska, M. Krell and D. E. Irish, *J. Electrochem. Soc.*, 1992, **139**, 3052.
- 27 P. C. Howlett, D. R. MacFarlane and A. F. Hollenkamp, *J. Power Sources*, 2003, **114**, 277.
- 28 D. Aurbach and Y. Cohen, *J. Electrochem. Soc.*, 1996, **143**, 3525.
- 29 M. L. Granvalet-Mancini, T. Hanrath and D. Teeters, *Solid State Ionics*, 2000, **135**, 283.
- 30 D. Aurbach, *J. Power Sources*, 2000, **89**, 206.
- 31 K. Tasaki, K. Kanda, T. Kobayashi, S. Nakamura and M. Ue, *J. Electrochem. Soc.*, 2006, **153**, A2192.
- 32 M. Arakawa, S.-I. Tobishima, Y. Nemoto and J.-I. Yamaki, *J. Power Sources*, 1993, **43–44**, 27.
- 33 K. Kanamura, H. Tamura, S. Shiraishi and Z.-I. Takehara, *J. Electroanal. Chem.*, 1995, **394**, 49.
- 34 S. Shiraishi, K. Kanamura and Z.-I. Takehara, *J. Electrochem. Soc.*, 1999, **146**, 1633.
- 35 J.-I. Yamaki, S.-I. Tobishima, K. Hayashi, K. Saito, Y. Nemoto and M. Arakawa, *J. Power Sources*, 1998, **74**, 219.
- 36 D. P. Barkey, R. H. Muller and C. W. Tobias, *J. Electrochem. Soc.*, 1989, **136**, 2199.
- 37 O. Crowther and A. C. West, *J. Electrochem. Soc.*, 2008, **155**, A806.
- 38 M. Z. Mayers, J. W. Kaminski and T. F. Miller, III, *J. Phys. Chem. C*, 2012, **116**, 26214.
- 39 C. Brissot, M. Rosso, J. N. Chazalviel, P. Baudry and S. Lascaud, *Electrochim. Acta*, 1998, **43**, 1569.
- 40 D. Aurbach, Y. Gofer and M. Ben-Zion, *J. Power Sources*, 1992, **39**, 163.
- 41 Y. Hanyu and I. Honma, *Surf. Sci. Rep.*, 2012, **2**, 453.
- 42 K. Okita, K.-I. Ikeda, H. Sano, Y. Iriyama and H. Sakaue, *J. Power Sources*, 2011, **196**, 2135.
- 43 Y.-S. Lee, J. H. Lee, J.-A. Choi, W. Y. Yoon and D.-W. Kim, *Adv. Funct. Mater.*, 2013, **23**, 1019.
- 44 K. Xu, *Chem. Rev.*, 2004, **104**, 4303.
- 45 R. Selim and P. Bro, *J. Electrochem. Soc.*, 1974, **121**, 1457.
- 46 D. Aurbach, M. L. Daroux, P. W. Faguy and E. Yeager, *J. Electrochem. Soc.*, 1987, **134**, 1611.
- 47 D. Aurbach, A. Zaban, A. Schechter, Y. Ein-Eli, E. Zinigrad and B. Markovsky, *J. Electrochem. Soc.*, 1995, **142**, 2873.
- 48 V. R. Koch and J. H. Young, *J. Electrochem. Soc.*, 1978, **125**, 1371.
- 49 I. Yoshimatsu, T. Hirai and J. Yamaki, *J. Electrochem. Soc.*, 1988, **135**, 2422.
- 50 K. M. Abraham, J. S. Foos and J. L. Goldman, *J. Electrochem. Soc.*, 1984, **131**, 2197.
- 51 Y. Geronov, B. Puresheva, R. V. Moshtev, P. Zlatilova, T. Kosev, Z. Staynov, G. Pistoia and M. Pasquali, *J. Electrochem. Soc.*, 1990, **137**, 3338.
- 52 J. Gao, M. A. Lowe, Y. Kiya and H. D. Abruna, *J. Phys. Chem. C*, 2011, **115**, 25132.
- 53 J. Yamaki, I. Yamazaki, M. Egashira and S. Okada, *J. Power Sources*, 2001, **102**, 288.
- 54 S. S. Zhang and C. A. Angell, *J. Electrochem. Soc.*, 1996, **143**, 4047.
- 55 Y. Matsuda, M. Morita, K. Yamada and K. Hirai, *J. Electrochem. Soc.*, 1985, **132**, 2538.

- 56 G. H. Newman, R. W. Francis, L. H. Gaines and B. M. Rao, *J. Electrochem. Soc.*, 1980, **127**, 2025.
- 57 C. Nanjundiah, J. L. Goldman, L. A. Dominey and V. R. Koch, *J. Electrochem. Soc.*, 1988, **135**, 2914.
- 58 D. H. Jang and S. M. Oh, *J. Electrochem. Soc.*, 1997, **144**, 3342.
- 59 S. Shiraishi, K. Kanamura and Z. Takehara, *Langmuir*, 1997, **13**, 3542.
- 60 K. Kanamura, H. Tamura, S. Shiraishi and Z. Takehara, *J. Electrochem. Soc.*, 1995, **142**, 340.
- 61 K. Naoi, M. Mori, Y. Naruoka, W. M. Lamanna and R. Atanasoski, *J. Electrochem. Soc.*, 1999, **146**, 462.
- 62 D. R. Macfarlane, M. Forsyth, P. C. Howlett, J. M. Pringle, J. Sun, G. Annat, W. Neil and E. I. Izgorodina, *Acc. Chem. Res.*, 2007, **40**, 1165.
- 63 N. Schweikert, A. Hofmann, M. Schulz, M. Scheuermann, S. T. Boles, T. Hanemann, H. Hahn and S. Indris, *J. Power Sources*, 2013, **228**, 237.
- 64 P. C. Howlett, D. R. MacFarlane and A. F. Hollenkamp, *Electrochem. Solid-State Lett.*, 2004, **7**, A97.
- 65 G. H. Lane, A. S. Best, D. R. MacFarlane, M. Forsyth, P. M. Bayley and A. F. Hollenkamp, *Electrochim. Acta*, 2010, **55**, 8947.
- 66 G. B. Appetecchi, G.-T. Kim, M. Montanino, M. Carewska, R. Marcilla, D. Mecerreyres and I. De Meatz, *J. Power Sources*, 2010, **195**, 3668.
- 67 A. Basile, A. F. Hollenkamp, A. I. Bhatt and A. P. O'Mullane, *Electrochem. Commun.*, 2013, **27**, 69.
- 68 J. O. Besenhard, M. W. Wagner, M. Winter, A. D. Jannakoudakis, P. D. Jannakoudakis and E. Theodoridou, *J. Power Sources*, 1993, **43–44**, 413.
- 69 S. B. Brummer, V. R. Koch and R. D. Rauh, in *Materials for Advanced Batteries*, ed. D. W. Murphy, J. Broadhead and B. C. H. Steel, 1980, Plenum Press, New York, p. 123.
- 70 S. Yoon, J. Lee, S.-O. Kim and H.-J. Sohn, *Electrochim. Acta*, 2008, **53**, 2501.
- 71 M. Ishikawa, M. Morita and Y. Matsuda, *J. Power Sources*, 1997, **68**, 501.
- 72 M. Ishikawa, S. Machino and M. Morita, *J. Electroanal. Chem.*, 1999, **473**, 279.
- 73 Y. Matsuda, M. Ishikawa, S. Yoshitake and M. Morita, *J. Power Sources*, 1995, **54**, 301.
- 74 J. K. Stark, Y. Ding and P. A. Kohl, *J. Electrochem. Soc.*, 2011, **158**, A1100.
- 75 K. Kanamura, S. Shiraishi and Z. Takehara, *J. Fluorine Chem.*, 1998, **87**, 235.
- 76 G. H. Lanea, A. S. Best, D. R. MacFarlane, M. Forsyth and A. F. Hollenkamp, *Electrochim. Acta*, 2010, **55**, 2210.
- 77 M. Morita, S. Oki and Y. Matsuda, *Electrochim. Acta*, 1992, **31**, 119.
- 78 R. Mogi, M. Inaba, S.-K. Jeong, Y. Iriyama, T. Abe and Z. Ogumi, *J. Electrochem. Soc.*, 2002, **149**, A1578.
- 79 N. Byrne, P. C. Howlett, D. R. MacFarlane and M. Forsyth, *Adv. Mater.*, 2005, **17**, 2497.
- 80 J. O. Besenhard, J. Gortler, P. Komenda and A. Paxinos, *J. Power Sources*, 1987, **20**, 253.
- 81 T. Hirai, I. Yoshimatsu and J. Yamaki, *J. Electrochem. Soc.*, 1994, **141**, 2300.
- 82 M. Mori, Y. Naruoka and K. Naoi, *J. Electrochem. Soc.*, 1998, **145**, 2340.
- 83 T. Inose, S. Tada, H. Morimoto and S. Tobishima, *J. Power Sources*, 2006, **161**, 550.
- 84 A. T. Ribes, P. Beaunier, P. Willmann and D. Lemordant, *J. Power Sources*, 1996, **58**, 189.
- 85 T. Osaka, T. Momma, Y. Matsumoto and Y. Uchida, *J. Electrochem. Soc.*, 1991, **144**, 1709.
- 86 M. Paunovic and M. Schlesinger, in *Fundamentals of electrochemical deposition*, John Wiley & Sons, 1998, ch. 10.
- 87 R. Akolkar, *J. Power Sources*, 2013, **232**, 23.
- 88 F. Ding, W. Xu, G. L. Graff, J. Zhang, M. Sushko, X. Chen, Y. Shao, M. H. Engelhard, Z. Nie, J. Xiao, X. Liu, P. V. Sushko, J. Liu and J.-G. Zhang, *J. Am. Chem. Soc.*, 2013, **135**, 4450.
- 89 A. M. Stephan, *Eur. Polym. J.*, 2006, **42**, 21.
- 90 F. B. Dias, L. Plomp and J. B. J. Veldhuis, *J. Power Sources*, 2000, **88**, 169.
- 91 K. M. Abraham and M. Alamgir, *Chem. Mater.*, 1991, **3**, 339.
- 92 L. Gao and D. D. Macdonald, *J. Electrochem. Soc.*, 1997, **144**, 1174.
- 93 S. Liu, N. Imanishi, T. Zhang, A. Hirano, Y. Takeda, O. Yamamoto and J. Yang, *J. Electrochem. Soc.*, 2010, **157**, A1092.
- 94 H. Wang, N. Imanishi, A. Hirano, Y. Takeda and O. Yamamoto, *J. Power Sources*, 2012, **219**, 22.
- 95 S. Liu, H. Wang, N. Imanishi, T. Zhang, A. Hirano, Y. Takeda, O. Yamamoto and J. Yang, *J. Power Sources*, 2011, **196**, 7681.
- 96 N.-S. Choi, B. Koo, J.-T. Yeon, K.-T. Lee and D.-W. Kim, *Electrochim. Acta*, 2011, **56**, 7249.
- 97 G. T. Kim, G. B. Appetecchi, F. Alessandrini and S. Passerini, *J. Power Sources*, 2007, **171**, 861.
- 98 F. Croce, G. B. Appetecchi, L. Persi and B. Scrosati, *Nature*, 1998, **394**, 456.
- 99 R. C. Agrawal and G. P. Pandey, *J. Phys. D: Appl. Phys.*, 2008, **41**, 223001.
- 100 B. Kumar and L. G. Scanlon, *J. Power Sources*, 1994, **52**, 261.
- 101 H.-M. Kao and C.-L. Chen, *Angew. Chem., Int. Ed.*, 2004, **116**, 998.
- 102 C.-S. Liao and W.-B. Ye, *J. Polym. Res.*, 2003, **10**, 241.
- 103 J. E. Weston and B. C. Steele, *Solid State Ionics*, 1982, **7**, 75.
- 104 M. Siekierski, P. Rzeszotarski and K. Nadara, *Solid State Ionics*, 2005, **176**, 2129.
- 105 C. C. Tambelli, A. C. Bloise, A. V. Rosario, E. C. Pereira, C. J. Magon and J. P. Donoso, *Electrochim. Acta*, 2002, **47**, 1677.
- 106 R. A. Vaia, S. Vasudevan, W. Krawiec, L. G. Scanlon and E. P. Giannelis, *Adv. Mater.*, 1995, **7**, 154.
- 107 L. Z. Fan, C. W. Nan and M. Li, *Chem. Phys. Lett.*, 2003, **369**, 698.
- 108 J. Xi, S. Miao and X. Tang, *Macromolecules*, 2004, **37**, 8592.
- 109 C.-W. Nan, L. Fan, Y. Lin and Q. Cai, *Phys. Rev. Lett.*, 2003, **91**, 266104.

- 110 J. Xi and X. Tang, *Electrochim. Acta*, 2005, **50**, 5293.
- 111 F. Marchioni, K. Star, E. Menke, T. Buffeteau, L. Servant, B. Dunn and F. Wudl, *Langmuir*, 2007, **23**, 11597.
- 112 J. S. Sakamoto, F. Wudl and B. Dunn, *Solid State Ionics*, 2001, **144**, 295.
- 113 S. Neuhold, D. J. Schroeder and J. T. Vaughey, *J. Power Sources*, 2006, **206**, 295.
- 114 R. S. Thompson, D. J. Schroeder, C. M. López, S. Neuhold and J. T. Vaughey, *Electrochim. Commun.*, 2011, **13**, 1369.
- 115 N.-S. Choi, Y. M. Lee, J. H. Park and J.-K. Park, *J. Power Sources*, 2003, **119–121**, 610.
- 116 N.-S. Choi, Y. M. Lee, K. Y. Cho, D.-H. Ko and J.-K. Park, *Electrochim. Commun.*, 2004, **6**, 1238.
- 117 Z.-I. Takehara, Z. Ogumi, Y. Uchimoto, K. Yasuda and H. Yoshida, *J. Power Sources*, 1993, **43–44**, 377.
- 118 N.-S. Choi, Y. M. Lee, W. Seol, J. A. Lee and J.-K. Park, *Solid State Ionics*, 2004, **172**, 19.
- 119 M. Wu, Z. Wen, Y. Liu, X. Wang and L. Huang, *J. Power Sources*, 2011, **196**, 8091.
- 120 L. C. Dejonghe and S. J. Visco, *et al.*, US20080113261-A1, 2008.
- 121 D. Aurbach, E. Zinigrad, H. Teller and P. Dan, *J. Electrochem. Soc.*, 2000, **147**, 1274.
- 122 M. S. Park and W. Y. Yoon, *J. Power Sources*, 2003, **114**, 237.
- 123 M. Rosso, T. Gobron, C. Brissot, J.-N. Chazalviel and S. Lascaud, *J. Power Sources*, 2001, **97–98**, 804.
- 124 C. Monroe and J. Newman, *J. Electrochem. Soc.*, 2003, **150**, A1377.
- 125 I. W. Seong, C. H. Hong, B. K. Kim and W. Y. Yoon, *J. Power Sources*, 2008, **178**, 769.
- 126 A. Zhamu, G. Chen, C. Liu, D. Neff, Q. Fang, Z. Yu, W. Xiong, Y. Wang, X. Wang and B. Z. Jang, *Energy Environ. Sci.*, 2012, **5**, 5701.
- 127 X. Ji, D.-Y. Liu, D. G. Prendiville, Y. Zhang, X. Liu and G. D. Stucky, *Nano Today*, 2012, **7**, 10.
- 128 R. Kanno, M. Murayama, T. Inada, T. Kobayashi, K. Sakamoto, N. Sonoyama, A. Yamada and S. Kondo, *Electrochim. Solid-State Lett.*, 2004, **7**, A455.
- 129 T. Pereira, R. Scaffaro, Z. Guo, S. Nieh, J. Arias and H. T. Hahn, *Adv. Eng. Mater.*, 2008, **10**, 393.
- 130 M. Ishikawa, Y. Takaki, M. Morita and Y. Matsuda, *J. Electrochem. Soc.*, 1997, **144**, L90.
- 131 G. Girishkumar, B. McCloskey, A. C. Luntz, S. Swanson and W. Wilcke, *J. Phys. Chem. C*, 2010, **1**, 2193.
- 132 A. Kraytsberg and Y. Ein-Eli, *J. Power Sources*, 2011, **196**, 886.
- 133 D. Capsoni, M. Bini, S. Ferrari, E. Quartarone and P. Mustarelli, *J. Power Sources*, 2012, **220**, 253.
- 134 H. Yamin, J. Penciner, A. Gorenstein, M. Elam and E. Peled, *J. Power Sources*, 1985, **14**, 129.
- 135 H. Yamin, A. Gorenstein, J. Penciner, Y. Sternberg and E. Peled, *J. Electrochem. Soc.*, 1988, **135**, 1045.
- 136 S.-E. Cheon, K.-S. Ko, J.-H. Cho, S.-W. Kim, E.-Y. Chin and H.-T. Kim, *J. Electrochem. Soc.*, 2003, **150**, A796.
- 137 Y. V. Milkaylik and J. R. Akridge, *J. Electrochem. Soc.*, 2004, **151**, A1969.
- 138 S. J. Visco and M.-Y. Chu, *US Pat.*, 6 025 094, 2000.
- 139 M.-Y. Chu, S. J. Visco and L. C. De Jonghe, *US Pat.*, 6 402 795, 2002.
- 140 J. Fu, *US Pat.*, 5 702 995, 1997.
- 141 J. Fu, *Solid State Ionics*, 1997, **96**, 195.
- 142 S. J. Visco, B. D. Katz, Y. S. Nimon and L. C. De Jonghe, *US Pat.*, 7 282 295, 2007.
- 143 N. Imanishi, S. Hasegawa, T. Zhang, A. Hirano, Y. Takeda and O. Yamamoto, *J. Power Sources*, 2008, **185**, 1392.
- 144 S. Hasegawa, N. Imanishi, T. Zhang, J. Xie, A. Hirano, Y. Takeda and O. Yamamoto, *J. Power Sources*, 2009, **189**, 371.
- 145 T. Zhang, N. Imanishi, S. Hasegawa, A. Hirano, J. Xie, Y. Takeda, O. Yamamoto and N. Sammes, *J. Electrochem. Soc.*, 2008, **155**, A965.
- 146 T. Zhang, N. Imanishi, S. Hasegawa, A. Hirano, J. Xie, Y. Takeda, O. Yamamoto and N. Sammes, *Electrochim. Solid-State Lett.*, 2009, **12**, A132.
- 147 T. Zhang, N. Imanishi, Y. Shimonishi, A. Hirano, Y. Takeda, O. Yamamoto and N. Sammes, *Chem. Commun.*, 2010, **46**, 1661.
- 148 Y. V. Milkaylik, *US Pat.*, 7 553 590, 2009.
- 149 Y. V. Milkaylik, *US Pat.*, 7 842 421, 2010.
- 150 D. Aurbach, E. Pollak, R. Elazari, G. Salitra, C. S. Kelley and J. Affinito, *J. Electrochem. Soc.*, 2009, **156**, A694.
- 151 X. Liang, Z. Wen, Y. Lin, M. Wu, J. Jin, H. Zhang and X. Wu, *J. Power Sources*, 2011, **196**, 9839.
- 152 S. S. Zhang and J. A. Read, *J. Power Sources*, 2012, **200**, 77.
- 153 S. S. Zhang, *Electrochim. Acta*, 2012, **70**, 344.
- 154 N. Liu, L. Hu, M. T. McDowell, A. Jackson and Y. Cui, *ACS Nano*, 2011, **5**, 6487.
- 155 R. Elazari, G. Salitra, G. Gershinsky, A. Garsuch, A. Pancehnko and D. Aurbach, *Electrochim. Commun.*, 2012, **14**, 21.
- 156 J. Hassoun, J. Kim, D.-J. Lee, H.-G. Jung, S.-M. Lee, Y. K. Sun and B. Scrosati, *J. Power Sources*, 2012, **202**, 308.
- 157 Y. Yan, Y.-X. Yin, S. Xin, J. Su, Y.-G. Guo and L.-J. Wan, *Electrochim. Acta*, 2013, **91**, 58.
- 158 R. Bhattacharyya, B. Key, H. Chen, A. S. Best, A. F. Hollenkamp and C. P. Grey, *Nat. Mater.*, 2010, **9**, 504.
- 159 S. Chandrashekhar, N. M. Trease, H. J. Chang, L.-S. Du, C. P. Grey and A. Jerschow, *Nat. Mater.*, 2012, **11**, 311.
- 160 M.-H. Ryou, D. J. Lee, J.-N. Lee, Y. M. Lee, J.-K. Park and J. W. Choi, *Adv. Energy Mater.*, 2012, **1**, 610.
- 161 H. Jin, Z. Li, L. Ju and Y. Xu, *ECS Electrochim. Lett.*, 2012, **1**, A59.
- 162 K. Sasajima, Y. Yamamoto, H. Munakata and K. Kanamura, 217th Electrochemical Society Meeting, 2010 (Abstract #356).
- 163 T. Gregory, R. J. Hoffman and R. C. Winterton, *J. Electrochem. Soc.*, 1990, **137**, 775.
- 164 D. Aurbach, Z. Lu, A. Schechter, Y. Gofer, H. Gizbar, R. Turgeman, Y. Cohen, M. Moshkovich and E. Levi, *Nature*, 2000, **407**, 724.
- 165 T. Reddy and D. Linden, *Linden's Handbook of Batteries*, McGraw, Hill, 4th edn, 2011.

- 166 P. Novak, R. Imhof and O. Haas, *Electrochim. Acta*, 1999, **45**, 351.
- 167 J. Muldoon, C. B. Bucur, A. G. Oliver, T. Sugimoto, M. Matsui, H. S. Kim, G. D. Allred, J. Zajicek and Y. Kotani, *Energy Environ. Sci.*, 2012, **5**, 5941.
- 168 E. Levi, Y. Gofer and D. Aurbach, *Chem. Mater.*, 2010, **22**, 860.
- 169 D. Aurbach, G. S. Suresh, E. Levi, A. Mitelman, O. Mizrahi, O. Chusid and M. Brunelli, *Adv. Mater.*, 2007, **19**, 4260.
- 170 Z. Lu, A. Schechter, M. Moshkovich and D. Aurbach, *J. Electroanal. Chem.*, 1999, **466**, 203.
- 171 Y. Liang, R. Feng, S. Yang, H. Ma, J. Liang and J. Chen, *Adv. Mater.*, 2011, **23**, 640.
- 172 S. Rasul, S. Suzuki, S. Yamaguchi and M. Miyayama, *Solid State Ionics*, 2012, **225**, 542.
- 173 Z. L. Tao, L. N. Xu, X. L. Gou, J. Chen and H. T. Yuan, *Chem. Commun.*, 2004, 2080.
- 174 D. Imamura, M. Miyayama, M. Hibino and T. Kudo, *J. Electrochem. Soc.*, 2003, **150**, A753.
- 175 Y. NuLi, J. Yang, J. Wang and Y. Li, *J. Phys. Chem. C*, 2009, **113**, 12594.
- 176 Y. NuLi, Y. Zheng, Y. Wang, J. Yang and J. Wang, *J. Mater. Chem.*, 2011, **21**, 12437.
- 177 O. Mizrahi, N. Amir, E. Pollak, O. Chusid, V. Marks, H. Gottlieb, L. Larush, E. Zinigrad and D. Aurbach, *J. Electrochem. Soc.*, 2008, **155**, A103.
- 178 D. Aurbach, H. Gizbar, A. Schechter, O. Chusid, H. E. Gottlieb, Y. Gofer and I. Goldberg, *J. Electrochem. Soc.*, 2002, **149**, A115.
- 179 J. H. Connor, W. E. Reid and G. B. Wood, *J. Electrochem. Soc.*, 1957, **104**, 38.
- 180 C. Liebenow, *J. Appl. Chem.*, 1997, **27**, 221.
- 181 D. Aurbach, A. Schechter, M. Moshkovich and Y. Cohen, *J. Electrochem. Soc.*, 2001, **148**, A1004.
- 182 M. Matsui, *J. Power Sources*, 2011, **196**, 7048.
- 183 A. P. Syvertsen, *PhD Dissertation*, Norwegian University of Science and Technology, 2012.
- 184 B. Peng, J. Liang, Z. Tao and J. Chen, *J. Mater. Chem.*, 2009, **19**, 2877.
- 185 F. Tang, T. Parker, H. F. Li, G. C. Wang and T. M. Lu, *J. Nanosci. Nanotechnol.*, 2007, **7**, 3239.
- 186 K. Zhang, C. Rossi, C. Tenailleau and P. Alphonse, *Appl. Phys. Lett.*, 2008, **92**, 063123.
- 187 T. S. Arthur, N. Singh and M. Matsui, *Electrochem. Commun.*, 2012, **16**, 103.
- 188 N. Singh, T. S. Arthur, C. Ling, M. Matsui and F. Mizuno, *Chem. Commun.*, 2013, **49**, 149.
- 189 <http://www.magpowersystems.com/>.
- 190 O. Sivakesavam and Y. V. R. K. Prasad, *Mater. Sci. Eng., A*, 2002, **323**, 270.
- 191 Y. Ma, N. Li, D. Li, M. Zhang and X. Huang, *J. Power Sources*, 2011, **196**, 2346.
- 192 W. Li, C. Li, C. Zhou, H. Ma and J. Chen, *Angew. Chem., Int. Ed.*, 2006, **118**, 6155.
- 193 D. J. Bradwell, H. Kim, A. H. C. Sirk and D. R. Sadoway, *J. Am. Chem. Soc.*, 2012, **134**, 1895.
- 194 D. P. Gregory, *Metal-air Batteries*, Mills & Boon Limited, London, 1972.
- 195 J.-S. Lee, S. T. Kim, R. Cao, N.-S. Choi, M. Liu, K. T. Lee and J. Cho, *Adv. Energy Mater.*, 2011, **1**, 34.
- 196 F. Cheng and J. Chen, *Chem. Soc. Rev.*, 2012, **41**, 2172.
- 197 J. R. Goldstein and B. Koretz, Proceedings of the 14th International Seminar on Primary and Secondary Battery Technology and Application, Deerfield Beach, Florida, 1995.
- 198 C. J. Lan, T. S. Chon, P. H. Lin and T. P. Perng, *J. New Mater. Electrochem. Syst.*, 2006, **9**, 27.
- 199 D. J. Mackinnon and J. M. Brannen, *J. Appl. Electrochem.*, 1982, **12**, 21.
- 200 K. I. PoPov, M. G. Pavlovic, M. D. Spasojevic and V. M. Nakic, *J. Appl. Electrochem.*, 1979, **9**, 533.
- 201 E. Frckowiak and M. Kiciak, *Electrochim. Acta*, 1988, **33**, 441.
- 202 C. Cachet, U. Stroder and R. Wiart, *Electrochim. Acta*, 1982, **27**, 903.
- 203 C. Cachet, B. Saidani and R. Wiart, *J. Electrochem. Soc.*, 1992, **139**, 644.
- 204 T. P. Dirkse, *J. Electrochem. Soc.*, 1981, **128**, 1412.
- 205 E. G. Gagnon, *J. Electrochem. Soc.*, 1986, **133**, 1989.
- 206 S. Szpak, C. J. Gabriel and T. Katan, *J. Electrochem. Soc.*, 1980, **127**, 1063.
- 207 G. D. Wilcox and P. J. Mitchell, *J. Power Sources*, 2007, **52**, 5407.
- 208 N. A. Hampson and A. J. S. McNeil, *J. Power Sources*, 1985, **15**, 61.
- 209 N. A. Hampson and A. J. S. McNeil, *J. Power Sources*, 1985, **15**, 245.
- 210 N. A. Hampson and A. J. S. McNeil, *J. Power Sources*, 1985, **15**, 261.
- 211 K. Bass, P. J. Mitchell, G. D. Wilcox and J. Smith, *J. Power Sources*, 1988, **24**, 21.
- 212 J. McBreen and E. Gannon, *J. Power Sources*, 1985, **15**, 169.
- 213 J. McBreen and E. Gannon, *Electrochim. Acta*, 1981, **26**, 1439.
- 214 K. Bass, P. J. Mitchell and G. D. Wilcox, *J. Power Sources*, 1991, **35**, 333.
- 215 J. McBreen and E. Gannon, *J. Electrochem. Soc.*, 1983, **130**, 1980.
- 216 J. W. Diggle and A. Damjanovic, *J. Electrochem. Soc.*, 1970, **117**, 65.
- 217 J. M. Wang, L. Zhang, C. Zhang and J. Q. Zhang, *J. Power Sources*, 2001, **102**, 39.
- 218 C. J. Lan, C. Y. Lee and T. S. Chin, *Electrochim. Acta*, 2007, **52**, 5407.
- 219 Y. Sharma, M. Aziz, J. Yusof and K. Kordes, *J. Power Sources*, 2001, **94**, 129.
- 220 J. Q. Kan, H. G. Xue and S. L. Mu, *J. Power Sources*, 1998, **74**, 113.
- 221 C. W. Lee, K. Sathiyanarayanan, S. W. Eom, H. S. Kim and M. S. Yun, *J. Power Sources*, 2006, **159**, 1474.
- 222 R. E. F. Einerhand, W. H. M. Visscher and E. Barendrecht, *J. Appl. Electrochem.*, 1988, **18**, 799.

- 223 V. S. Muralidharan and K. S. Rajagopalan, *J. Electroanal. Chem.*, 1978, **94**, 21.
- 224 V. Ravindran and V. S. Muralidharan, *J. Power Sources*, 1995, **55**, 237.
- 225 C. Chakkaravarthy, A. K. A. Waheed and H. V. K. Udupa, *J. Power Sources*, 1981, **6**, 203.
- 226 L. F. Urry, *US Pat.*, 6,022,639, 1996.
- 227 T. I. Devyatkina, Y. L. Gunko and M. G. Mikhaleko, *Russ. J. Appl. Chem.*, 2001, **74**, 1122.
- 228 C. W. Lee, K. Sathiyaanarayanan, S. W. Eom and M. S. Yun, *J. Power Sources*, 2006, **160**, 1436.
- 229 C. Zhang, J. M. Wang, L. Zhang, J. Q. Zhang and C. N. Cao, *J. Appl. Electrochem.*, 2001, **31**, 1049.
- 230 J. Dobryszycki and S. Biallozor, *Corros. Sci.*, 2001, **43**, 1309.
- 231 T. G. Company, *World Pat.*, WO01/890650, 2002.
- 232 T. Burchardt, *World Pat.*, WO2006/538111, 2002.
- 233 S. Müller, F. Holzer and O. Haas, *J. Appl. Electrochem.*, 1998, **28**, 895.
- 234 R. Othman, W. J. Basirun, A. H. Yahaya and A. K. Arof, *J. Power Sources*, 2001, **103**, 34.
- 235 I. Arise, Y. Fukunaka and F. R. McLarnon, *J. Electrochem. Soc.*, 2006, **153**, A69.
- 236 J. Hendrikx, A. Van Der Putten, W. Visscher and E. Barendrecht, *Electrochim. Acta*, 1984, **29**, 81.
- 237 W.-J. Peng and Y.-Y. Wang, *J. Cent. South Univ. Technol.*, 2007, **14**, 37.
- 238 X. G. Zhang, *J. Power Sources*, 2006, **163**, 591.
- 239 C.-C. Yang and S.-J. Lin, *J. Power Sources*, 2002, **112**, 174.
- 240 G. Coates, N. A. Hampson, A. Marshall and D. F. Porter, *J. Appl. Electrochem.*, 1974, **4**, 75.
- 241 N. C. Tang, *US Pat.*, 6,221,527, 1998.
- 242 <http://www.powergenix.com/>.
- 243 A. K. Shukla, S. Venugopalan and H. Hariprakash, *J. Power Sources*, 2001, **100**, 125.
- 244 M. Geng and D. O. Northwood, *Int. J. Hydrogen Energy*, 2003, **28**, 633.
- 245 H. Iwanaga, M. Fujii and S. Takeuchi, *J. Cryst. Growth*, 1998, **183**, 190.
- 246 M. Y. Abyaneh, J. Hendrikx, W. Visscher and E. Barendrecht, *J. Electrochem. Soc.*, 1982, **129**, 2654.
- 247 Y. F. Yuan, J. P. Tu, H. M. Wu, B. Zhang, X. H. Huang and X. B. Zhao, *J. Electrochem. Soc.*, 2006, **153**, A1719.
- 248 J. Z. Wu, J. P. Tua, Y. F. Yuan, M. Ma, X. L. Wang, L. Zhang, R. L. Li and J. Zhang, *J. Alloys Compd.*, 2009, **479**, 624.
- 249 Y. F. Yuan, J. P. Tu, S. Y. Guo, J. B. Wu, M. Ma, J. L. Yang and X. L. Wang, *Appl. Surf. Sci.*, 2008, **254**, 5080.
- 250 A. Renuka, A. Veluchamy and N. Venkatakrishnan, *J. Appl. Electrochem.*, 1992, **22**, 182.
- 251 R. Shrivikumar, G. Paruthimal Kalaigan and T. Vasudevan, *J. Power Sources*, 1998, **75**, 90.
- 252 D. Coates, E. Ferreira and A. Charkey, *J. Power Sources*, 1997, **65**, 109.
- 253 D. E. G. Gagnon and Y. M. Wang, *J. Electrochem. Soc.*, 1987, **134**, 2091.
- 254 Y. F. Yuan, J. P. Tu, H. M. Wu, Y. Li, D. Q. Shi and X. B. Zhao, *J. Power Sources*, 2006, **159**, 357.
- 255 H. Huang, L. Zhang, W. K. Zhang, Y. P. Gan and H. Shao, *J. Power Sources*, 2008, **184**, 663.
- 256 S.-H. Lee, C.-W. Yi and K. Kim, *J. Phys. Chem. C*, 2011, **115**, 2572.
- 257 F. R. McLarnon and E. J. Cairns, *J. Electrochem. Soc.*, 1991, **138**, 645.
- 258 F. Sanehiro and I. Kenji, *Japan Pat.*, 61,281,461, 1986.
- 259 J. L. Yang, Y. F. Yuan, H. M. Wu, Y. Li, Y. B. Chen and S. Y. Guo, *Electrochim. Acta*, 2010, **55**, 7050.
- 260 M. Ma, J. P. Tu, Y. F. Yuan, X. L. Wang, K. F. Li, F. Mao and Z. Y. Zen, *J. Power Sources*, 2008, **179**, 395.
- 261 Z. Yang, J. Zhang, M. C. W. Kintner-Meyer, X. Lu, D. Choi, J. P. Lemmon and J. Liu, *Chem. Rev.*, 2001, **111**, 3577.
- 262 J. Kummer and N. Weber, *U.S. Pat.*, 3,413,150, 1968.
- 263 B. Dunn, H. Kamath and J.-M. Tarascon, *Science*, 2011, 334–928.
- 264 G. Yamaguchi and K. Suzuki, *Bull. Chem. Soc. Jpn.*, 1968, **41**, 93.
- 265 M. Bettman and C. Peters, *J. Phys. Chem.*, 1969, **73**, 1774.
- 266 S. Tan, *J. Mater. Sci.*, 1977, **12**, 1058.
- 267 J. Hwang, S. Bae and M. Kim, *Ceramist*, 2012, 15–45.
- 268 A. Ray and E. Subbarao, *Mater. Res. Bull.*, 1975, **10**, 583.
- 269 P. Morgan, *Mater. Res. Bull.*, 1976, **11**, 233.
- 270 T. Takahashi and K. Kuwabara, *J. Appl. Electrochem.*, 1980, **10**, 291.
- 271 A. Pekarsky and P. S. Nicholson, *Mater. Res. Bull.*, 1980, **15**, 1517.
- 272 T. Mathews, *Mater. Sci. Eng., B*, 2000, **78**, 39.
- 273 R. Subasri, T. Mathews, O. M. Sreedharan and V. S. Raghunathan, *Solid State Ionics*, 2003, **158**, 199.
- 274 S. Heavens, *J. Mater. Sci.*, 1988, **23**, 3515.
- 275 A. Virkar, G. Tennenhouse and R. Gordon, *J. Am. Ceram. Soc.*, 1974, **57**, 508.
- 276 A. Eccleston, M. Robins, S. Bhavaraju, Y. Kim, W. Koh, J. Chae, J. Kim, PRIME 2012, Abstract #, 1875 (2012).
- 277 A. Hayashi, K. Noi, A. Sakuda and M. Tatsumisago, *Nat. Commun.*, 2012, **3**, 856.
- 278 J. Coetzer, *J. Power Sources*, 1986, **18**, 377.
- 279 J. Prakash, L. Redey and D. Vissers, *J. Electrochem. Soc.*, 2000, **147**, 502.
- 280 P. Moseley, R. Bones, D. Teagle, B. Bellamy and R. Hawes, *J. Electrochem. Soc.*, 1989, **136**, 1361.
- 281 E. Peled, D. Golodnitsky, H. Mazor and S. Avshalomov, *J. Power Sources*, 2011, **196**, 6835.
- 282 Q. Sun, Y. Yang and Z.-W. Fu, *Electrochim. Commun.*, 2012, **16**, 22.
- 283 S. K. Das, S. Xu and L. A. Archer, *Electrochim. Commun.*, 2013, **27**, 59.
- 284 A. Hayashil, K. Noi, A. Sakuda and M. Tatsumisago, *Nat. Commun.*, 2012, **3**, 856.
- 285 J.-G. Zhang, P. G. Bruce and X. G. Zhang, in *Handbook of Battery Materials*, ed. C. Daniel and J. O. Bessenhard, 2011, Wiley-VCH Verlag & Co. KGaA, Weinheim, Germany, ch. 22.
- 286 S. Yang and H. Knickle, *J. Power Sources*, 2002, **112**, 162.